



Antioxidant, Antimicrobial, Anticorrosion and Molecular docking studies on *Alpinia calcarata* Rosc., rhizome and leaf extracts

M. Jisha¹, N. H. Zeinul Hukuman¹, P. Leena^{1,2} and V. P. Nair^{3*}

¹Department of Post Graduate Studies and Research in Chemistry, Sir Syed College, Taliparamba, Kannur, Kerala, India. 670142

²Department of Chemistry, Govt. Brennen College, Thalassery, Kannur, Kerala, India. 670106

³Department of Biology, Health Sciences Division, GVHSS Payyoli, Thikkoti P.O, Kozhikode, Kerala, India. 673529

* Corresponding author E mail : vinayanpnair@gmail.com

Received 10 Nov 2020,
Revised 09 Feb 2021,
Accepted 15 Feb 2021

Keywords

- ✓ *Alpinia calcarata*
- ✓ GC MS analysis
- ✓ Antioxidant activity
- ✓ Corrosion inhibition
- ✓ Computational studies
- ✓ Antimicrobial activity
- ✓ Molecular docking

vinayanpnair@gmail.com
Phone: +91 9446956052

Abstract

Alpinia calcarata Rosc., belonging to Zingiberaceae has been investigated by GC-MS analysis for phytochemicals. Highest total phenolic content (TPC) was found in acetone extract and highest total flavonoid content (TFC) was in methanol extract of leaves. Acetone extract of leaves and rhizome exhibited high DPPH radical scavenging activity and leaf extracts are more active than rhizome based on IC₅₀. Experimental studies on antioxidant activity were supported by theoretical studies of selected components of the plant. Plant extract has been investigated as corrosion inhibitor for mild steel in 1M HCl. Corrosion rates were studied at 303K, 313K and 323 K by weight loss method at varying inhibitor concentrations. It shows maximum inhibition efficiency of 90.1% for leaves and 92% for rhizome at 300ppm inhibitor concentration. SEM, FT-IR and adsorption studies supported the inhibitory mechanism and surface morphology study. Antimicrobial (Well diffusion method) and molecular docking studies helped to reveal the inhibitory potential of phytochemicals.

1. Introduction

Alpinia calcarata Rosc., belonging to Zingiberaceae commonly known as greater galangal in English and *rasna* in Sanskrit, is a slender, rhizomatous herb often cultivated in East and South India, Sri Lanka, China and Malaysia. It has white flowers, variegated with red and yellow in pyramidal panicles [1,2]. The rhizomes are used in India, Sri Lanka and China for its medicinal uses such as treatment of bronchitis, cough, respiratory ailments, diabetics, asthma and arthritis [1]. *Alpinia calcarata* is a perennial herb with non-tuberous pungent rootstock. Its rhizomes showed antinociceptive activities. The rhizome extract of *A. calcarata* is used as an expectorant in the treatment of bronchitis and asthma; for purifying blood; stimulating digestion and improving voice [3,4]. *A. calcarata* is an important constituent of the polyherbal formulation, "Maharasnadi Kashayam" recommended by Ayurvedic medical practitioners for the treatment of arthritic conditions [5]. The preliminary phytochemical investigations on rhizomes of AC showed the presence of flavanoids, alkaloids, terpenoids, steroids, phenol, tannin, saponins, proteins and carbohydrates [6,7,8]. Various workers had isolated various compounds from the rhizome and leaves of *A. calcarata* from different parts of the world [1,9,10,11,12,13]. Antioxidant and antimicrobial studies reported are only basic studies on rhizome and

leaves [1,8,14,15,16,17,18]. No studies have been conducted regarding anticorrosive potential, computational studies on plant components regarding antioxidant potential and molecular docking. Hence a detailed study has been carried out.

Materials and Methods

2.1/ Plant material

Fresh plants of *A.calcarata* were collected from near Sir Syed college campus, Kannur, North Kerala, S.India, aerial leaves and rhizomes were washed shade dried and made into fine powder using mixer grinder and powder were kept in air tight bottles with proper labelling. Powdered rhizome and leaves were extracted using petroleum ether, acetone, methanol and water in increasing order of polarity using soxhlet apparatus until all the constituents were completely eluted. The extracts were filtered, evaporated to dry and used for further studies. For corrosion inhibition studies and antimicrobial studies rhizome and leaf powder were extracted with methanol in Soxhlet apparatus.

2.2/ GC- MS analysis

GC-MS analysis of rhizome and leaf extracts were carried out using Thermo Scientific Trace 1300 gas chromatograph equipped with ISD -QD Mass spectrometer with TG -5MS column (30m ×0.25 mm ×0.25 μm). Helium gas (99.99%) was the carrier gas at constant flow rate 1ml / mt and an injection volume of 1μl was employed (split ratio 1:8). Injection port temperature was 280⁰C and ion source temperature was 200⁰C. Oven temperature was programmed from 70⁰C for 3 mnts with increase of 10⁰C/mnt to 200⁰C with a hold time of 2 minutes and total GC running time 30 minutes. The components in the extract were identified based on mass spectra of the latest NIST library data.

2.3/ Determination of total phenolics (TPC) and total flavonoids (TFC)

The total phenolic contents (TPC) of selected plant parts were determined by Folin Ciocalteu's method (Hagerman *et. al.*) [19]. Accordingly, 100 mg of the extract of the sample was weighed accurately and dissolved in 100ml of triple distilled water. 1 ml of this solution was transferred to a test tube, then 0.5 ml of 2N of the Folin Ciocalteu reagent and 1.5 ml of 20% of Na₂CO₃ solution was added and ultimately the volume was made up to 8ml with TDW followed by vigorous shaking and finally allowed to stand for 2 hrs after which the absorbance was taken at 765 nm. These data were used to estimate the total phenolic content using a standard calibration curve obtained from various diluted concentrations of gallic acid. The total flavonoid contents (TFC) were determined by aluminium chloride colorimetric assay with slight modifications described by Zhishen *et. al.*, [20]. Accordingly, 0.5ml of approximately diluted (2mg/2ml) sample solution was mixed with 2ml of distilled water and subsequently with 0.15 ml of 5 % NaNO₂ solution. After 6 minutes 0.15ml of 10% AlCl₃ solution was added and allowed to stand for 6 minutes. Then 2 ml of 4% NaOH was added to the mixture to bring the final volume to 5ml and then the mixture was thoroughly mixed and allowed to stand for another 15 minutes. Absorbance of the mixture was determined at 510nm vs. water as blank. The analysis was performed in triplicates and the content of flavonoids in extracts was expressed in terms of rutin equivalent (mg of RU/g of extract).

2.4/Chemicals used in antioxidant study

The major chemicals used in the study were DPPH (1,1diphenyl – 2 – picrylhydrazyl) - Sigma Chemicals (USA), Potassium ferricyanide [K₃Fe (CN) ₆] – Loba Chemie Pvt. Ltd. (India) and Ascorbic acid - SD Fine Chem. Ltd. (India). Other chemicals and solvents used for extraction were of analytical grade.

2.5/DPPH free radical scavenging activity

The DPPH free radical scavenging activity has been carried out by the method described by Braca *et al.*, [21]. 100 – 600 µg/ml of plant extract was added to 3 ml of a 0.004 % ethanol solution of DPPH. After 30 minutes, absorbance at 517 nm was determined and the percentage inhibition activity was calculated by formula $[(A_0 - A_1) / A_0] \times 100$, where A_0 is the absorbance of the control (DPPH solution) and A_1 is the absorbance of the extract / standard. The inhibition curves were prepared and IC_{50} values were calculated. Ascorbic acid was used as standard.

2.6/Reducing power assay

The reducing power was determined as described by Oyaizu [22]. By measuring the absorbance of Perl's Prussian blue complex, the reduction of Fe^{3+} to Fe^{2+} is determined. Extracts with concentrations 50 – 250 µg in 1 ml of distilled water were mixed with phosphate buffer (2.5 ml, 0.2 M, pH 6.6) and potassium ferricyanide [$K_3Fe(CN)_6$] (2.5 ml, 1 %). The incubated mixture (50°C for 20 minutes) was mixed with 2.5 ml trichloro acetic acid (10%), which was then centrifuged at 3000 rpm (10 minutes). To the supernatant (2.5 ml), distilled water (2.5 ml) and $FeCl_3$ (0.5 ml, 0.1 %) was added and the absorbance was measured at 700 nm. Reducing power increases with increase in absorbance of the reaction mixture. The standard used was ascorbic acid.

2.7/Total antioxidant capacity (Phosphomolybdenum assay)

The total antioxidant capacity by phosphomolybdenum method was carried out as described by Prieto *et al.*, [23]. 3 ml of reagent solution (0.6 M sulphuric acid, 28 mM sodium phosphate and 4 mM ammonium molybdate) and 0.3 ml extract was combined. After incubation of the reaction solution (95°C for 90 min), the absorbance of the solution was measured at 695 nm using a UV – visible spectrophotometer (Shimadzu, 1601) against blank (Methanol (0.3ml.)) after cooling at room temperature. The antioxidant activity is given as the number of ascorbic acid equivalents.

2.8/Statistical analysis

The results are given as mean \pm standard deviation (SD) (triplicate experiments). One – way ANOVA followed by student's t- test were performed using Graph Pad Prism software version 7.02. Differences were considered significant at a level of $P < 0.05$. IC_{50} was calculated using Graph Pad Prism 7.02 software.

2.9/Corrosion inhibition study material

Mild steel specimens of size $2 \times 1.8 \text{ cm}^2$ were the test specimens. Prior to the measurements test specimens were treated as per standard methods. Weight of the samples were taken using four digit electronic balance (Shimadzu AAY220). The concentration ranges of the inhibitors were 100, 150, 200, 250 and 300 ppm in 1M HCl prepared from analytical grade HCl (Merck) using double distilled water.

2.10/Gravimetric measurements

Pre weighed steel samples immersed in blank solution of 1M HCl containing different concentrations of inhibitor (100 ppm, 150 ppm, 200 ppm, 250 ppm and 300 ppm) for 6 hrs are subjected to gravimetric measurements at 303K, 313 K and 323K temperatures. Withdrawn steel specimens were carefully rinsed with double distilled water, cleaned with acetone, dried and weighed.

2.11/Computational studies

Full geometry optimization of the inhibitors were performed using DFT (density functional theory) with Beck's three - parameter exchange functional along with Lee-Yang-Par non local correlation functional

(B3LYP) with 6-311 G (d,p) basic set using the Gaussian 09 programme package. Energy of the highest occupied molecular orbital (E_{HOMO}), energy of the lowest unoccupied molecular orbital (E_{LUMO}), ΔE (HOMO - LUMO energy gap), dipole moment (μ), total energy (TE), electronegativity (χ), hardness (η), the number of transferred electrons (ΔN) etc., are identified.

2.12/Antimicrobial study - test organisms

One fungal species, *Candida albicans* (ATCC10231), two gram negative bacteria, *Klebsiella pneumoniae* (ATCC13883) & *Pseudomonas aeruginosa* (ATCC 27853), and two gram positive bacteria, *Streptococcus mutans* (MTCC890) & *Staphylococcus aureus* (ATCC 25923) were used in the investigation.

2.13/Antifungal activity - Agar well diffusion method

Potato dextrose agar plates were prepared and overnight grown *Candida albicans* was swabbed. Wells of approximately 10 mm was bored using a well cutter and samples of different concentration was added, the zone of inhibition was measured after overnight incubation and compared with that of standard antimycotic (Clotrimazole).

2.14/ Antibacterial activity - Agar well diffusion method

The medium was prepared by dissolving 33.8 g of the commercially available Muller Hinton Agar Medium (HiMedia) in 1000ml of distilled water. The dissolved medium was autoclaved at 15 lbs pressure at 121°C for 15 minutes. The autoclaved medium was mixed well and poured onto 100 mm petriplates (25-30ml/plate) while still molten. One litre of nutrient broth was prepared by dissolving 13 g of commercially available nutrient medium (HiMedia) in 1000ml distilled water and boiled to dissolve the medium completely. The medium was dispensed as desired and sterilized by autoclaving at 15 lbs pressure (121°C) for 15 minutes. Streptomycin was used as standard antibacterial agent with a concentration of 20 μ g / ml. Petriplates containing 20ml Muller Hinton Agar Medium were seeded with bacterial culture of *Pseudomonas aeruginosa*, *Klebsiella pneumoniae*, *Streptococcus mutans* and *Staphylococcus aureus* (growth of culture adjusted according to McFards Standard, 0.5%). Wells of approximately 10mm was bored using a well cutter and sample of 25, 50, and 100 μ g/ml concentrations were added. The plates were then incubated at 37°C for 24 hours. The antibacterial activity was assayed by measuring the diameter of the inhibition zone formed around the well [24]. Streptomycin was used as a positive control.

2.15/Molecular docking studies

The 3D structure of penicillin-binding protein 3 (PDB ID: 3OC2) from *Pseudomonas aeruginosa* , glycerol dehydratase - cyanocobalamin complex (PDB ID: 1IWP) from *Klebsiella pneumoniae*, Streptococcus mutans inorganic pyrophosphatase (PDB ID: 1I74) from *Streptococcus mutans*, penicillin binding protein 2a (PDB ID: 1VQQ) from methicillin resistant *Staphylococcus aureus* and geranylgeranyltransferase-1 (PDB ID: 3DRA) from *Candida albicans* were downloaded from the PDB site (www.rcsb.org). Water molecules were removed from the protein and hydrogen atoms were added. The prepared ligands which were optimized with Gaussian 09 were docked using Autodock 4.2 software. The docked ligands were scored using high affinity and the best pose was identified which were used for further studies. 3D pose of the bound ligand is visualized using Pymol. The active binding site in the target proteins were determined using 3D ligand site web server (www.sbg.bio.ic.ac.uk/3dligandsite).

3. Results and discussion

3.1/GC-MS analysis of *A. calcarata* rhizome and leaves

The GC-MS chromatogram and phytochemicals identified from methanol and acetone extract of rhizome and methanol extract of leaves are provided in Figures 1, 2, 3 and Tables 1, 2 and 3 respectively. Twenty-three phytochemicals were identified from the methanol extract and fifty from the acetone extract of rhizome and thirty-three compounds from the methanol extract of leaves. Dinorlabdanic diterpenoids (*E*)-labda-8(17), 12-diene-15, 16-dial and (*E*)-15, 16-dinorlabda-

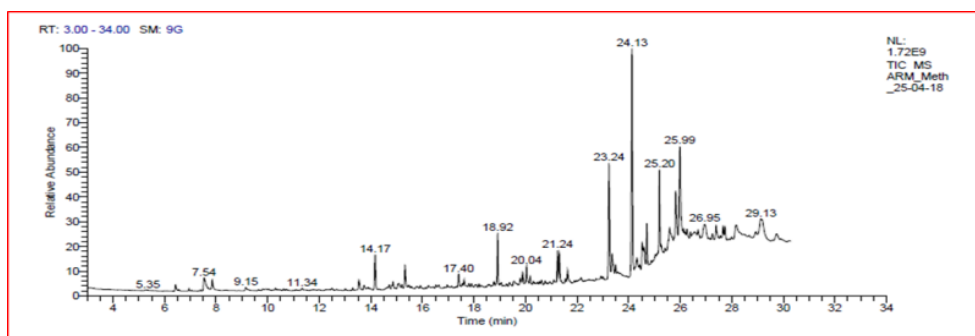


Figure 1. GC MS chromatogram of methanol extract of rhizome of *A. calcarata*

Table 1. Phytochemicals identified in the methanol extract of rhizome of *A. calcarata*

No.	RT	Name of compound	Molecular formula	MW	Peak area %
1.	7.53	Benzofuran 2,3 dihydro	C ₈ H ₈ O	120	1.4
2.	7.85	Benzyl acetone	C ₁₀ H ₁₂ O	148	0.69
3.	9.15	2-Methoxy-4-vinylphenol	C ₉ H ₁₀ O ₂	150	0.25
4.	9.64	1,2-Cyclohexanediol, 1-methyl-4-(1-methylethenyl)-	C ₁₀ H ₁₈ O ₂	170	0.04
5.	9.80	Phenol, 2,6-dimethoxy-	C ₈ H ₁₀ O ₃	154	0.12
6.	13.74	4-(1-Hydroxyallyl)-2-methoxyphenol	C ₁₀ H ₁₂ O ₃	180	0.41
7.	14.17	Carotol	C ₁₅ H ₂₆ O	222	2.27
8.	14.86	Daucol	C ₁₅ H ₂₆ O ₂	238	0.59
9.	17.4	Ambrial	C ₁₆ H ₂₆ O	234	0.81
10.	19.06	4aR,5S)-1-Hydroxy-4a,5-dimethyl-3-(propan-2-ylidene)- 4,4a,5,6 -tetrahydronaphthalen- 2(3H)- one	C ₁₀ H ₁₈ O ₂	232	0.32
11.	19.89	Benzene, 1,3-dimethoxy-5- (2-phenylethenyl)-, (<i>E</i>)-	C ₁₆ H ₁₆ O ₂	240	0.72
12.	20.04	(<i>E</i>)-15,16-Dinorlabda-8(17),11-dien-13-one	C ₁₈ H ₂₈ O	260	1.28
13.	21.24	9,12-Octadecadienoic acid (<i>Z,Z</i>)-, methyl ester	C ₁₉ H ₃₄ O ₂	294	1.75
14.	21.31	trans-13-Octadecenoic acid, methyl ester	C ₁₉ H ₃₆ O ₂	296	1.83
15.	21.64	Octadecanoic acid, methyl ester	C ₁₉ H ₃₈ O ₂	298	1.07
16.	22.17	(<i>E</i>)-Labda-8(17),12-diene-15,16-dial	C ₂₀ H ₃₀ O ₂	302	0.37
17.	23.24	Benzene, 1,3-dimethoxy-5- [(1 <i>E</i>)-2-phenylethenyl]-	C ₁₆ H ₁₆ O ₂	240	8.05
18.	23.36	2-Methyl-3,5-dinitrophenyl á-phenylpropionate	C ₁₆ H ₁₄ N ₂ O ₆	330	2.15
19.	24.13	1H-Imidazole, 4,5-dihydro-2-(phenylmethyl)-	C ₁₀ H ₁₂ N ₂	160	15.14
20.	25.20	3-Heptanone, 5-hydroxy-1,7-diphenyl-	C ₁₉ H ₂₂ O ₂	282	4.82
21.	25.99	4,6-Heptadien-3-one, 1,7-diphenyl-	C ₁₉ H ₁₈ O	262	7.46
22.	29.14	Stigmast-4-en-3-one, (2 <i>S</i>)-	C ₂₉ H ₄₈ O	412	2.96
23.	29.74	Stigmasterol	C ₂₉ H ₄₈ O	412	0.88

Table 2. Phytocompounds identified in the acetone extract of rhizome of *A. calcarata*

Sl.No	RT	Name of compound	Molecular formula	MW	Peak area %
1.	3.08	2-Pentanone, 4-hydroxy-4-methyl-	C ₆ H ₁₂ O ₂	116	0.52
2.	3.42	2-Pentanone, 4-amino-4-methyl-	C ₆ H ₁₃ NO	115	1.77
3.	4.60	1,3-Dioxolane-4-methanol, 2,2-dimethyl-, (S)-	C ₆ H ₁₂ O ₃	132	0.54
4.	5.44	α-Pinene	C ₁₀ H ₁₆	136	0.02
5.	5.76	Glycerin	C ₃ H ₈ O ₃	92	0.78
6.	6.24	Isopropyl acetate	C ₅ H ₁₀ O ₂	102	0.14
7.	6.83	Eucalyptol	C ₁₀ H ₁₈ O	154	0.46
8.	7.37	2-Pyrrolidinone, 1-methyl-	C ₅ H ₉ NO	99	0.89
9.	8.57	Fenchone	C ₁₀ H ₁₆ O	152	0.01
10.	9.52	4-Piperidinone, 2,2,6,6-tetramethyl-	C ₉ H ₁₇ NO	155	0.36
11.	12.29	α-Terpineol	C ₁₀ H ₁₈ O	154	0.06
12.	12.74	1,3-Dioxolane-4,5-dimethanol, 2,2-dimethyl-, (4R-trans)-	C ₇ H ₁₄ O ₄	162	1.5
13.	13.85	Benzofuran, 2,3-dihydro	C ₈ H ₈ O	120	1.22
14.	17.18	2-Methoxy-4-vinylphenol	C ₉ H ₁₀ O ₂	150	0.28
15.	18.73	Phenol, 2,6-dimethoxy-	C ₈ H ₁₀ O ₃	154	0.04
16.	18.93	3-Buten-2-one, 4-phenyl-	C ₁₀ H ₁₀ O	146	0.05
17.	19.43	α-copaene	C ₁₅ H ₂₄	204	0.10
18.	22.14	1,2-Propanediol, 3-(tetradecyloxy)-	C ₁₇ H ₃₆ O ₃	288	0.42
19.	22.65	2-Propenoic acid, 3-phenyl-	C ₉ H ₈ O ₂	148	0.98
20.	23.57	8,11,14-Eicosatrienoic acid, methyl ester, (Z,Z,Z)	C ₂₁ H ₃₆ O ₂	320	0.46
21.	24.85	2-Oxabicyclo[2.2.2]octan-6-ol, 1,3,3-trimethyl-	C ₁₀ H ₁₈ O ₂	170	0.62
22.	27.15	3',5'-Dimethoxyacetophenone	C ₁₀ H ₁₂ O ₃	180	0.82
23.	27.77	Carotol	C ₁₅ H ₂₆ O	222	1.01
24.	28.45	Daucol	C ₁₅ H ₂₆ O ₂	238	0.09
25.	28.81	Longifolenaldehyde	C ₁₅ H ₂₄ O	220	0.68
26.	28.96	cis-Dodec-5-enal	C ₁₂ H ₂₂ O	182	0.42
27.	29.55	6-epi-shyobunol	C ₁₅ H ₂₆ O	222	0.25
28.	29.80	Alloaromadendrene oxide-(1)	C ₁₅ H ₂₄ O	220	0.27
29.	29.92	Ambrial	C ₁₆ H ₂₆ O	234	2.98
30.	30.16	Ingol 12 –acetate	C ₂₂ H ₃₂ O ₇	408	0.98
31.	30.40	1-Heptatriacotanol	C ₃₇ H ₇₆ O	536	0.63
32.	30.59	α-Cyclocostunolide	C ₁₅ H ₂₀ O ₂	232	0.82
33.	30.67	Copalol	C ₃₀ H ₅₀ O	290	0.39
34.	30.74	n- Hexadecanoic acid	C ₁₆ H ₃₂ O ₂	256	2.33
35.	30.94	(E)-15,16-Dinorlabda-8(17),11-dien-13-one	C ₁₈ H ₂₈ O	260	0.52
36.	31.01	2,2,6,7-Tetramethyl-10-oxatricyclo[4.3.1.0(1,6)]decan-5-ol	C ₁₃ H ₂₂ O ₂	210	0.48
37.	31.15	4,8,13-Cyclotetradecatriene-1,3-diol, 1,5,9-trimethyl-12-(1-methylethyl)-	C ₂₀ H ₃₄ O ₂	306	0.47
38.	31.49	Lup-20(29)-en-3-ol, acetate, (3α)-	C ₃₂ H ₅₂ O ₂	468	11.36
39.	32.27	1H-Imidazole, 4,5-dihydro-2-(phenylmethyl)-	C ₁₀ H ₁₂ N ₂	160	0.58
40.	32.64	(E)-Labda-8(17),12-diene-15,16-dial	C ₂₀ H ₃₀ O ₂	302	1.76
41.	32.78	ç-Sitosterol	C ₂₉ H ₅₀ O	414	2.64
42.	32.91	(E)-15,16-Dinorlabda-8(17),12-dien-14-al	C ₁₈ H ₂₈ O	260	1.85
43.	33.20	Eicosanal	C ₂₀ H ₄₀ O	296	2.39
44.	33.39	4H-1-Benzopyran-4-one, 2,3-dihydro-5,7-dihydroxy-2-phenyl-, (S)	C ₁₅ H ₁₂ O ₄	256	9.39
45.	33.54	7-Hydroxy-5-methoxyflavan	C ₁₆ H ₁₆ O ₃	256	0.09
46.	34.08	Naringenin	C ₁₅ H ₁₂ O ₅	272	2.59
47.	34.47	Villosin	C ₂₀ H ₂₈ O ₂	300	1.16
48.	35.02	5-Hydroxy-7-methoxyflavanone	C ₁₆ H ₁₄ O ₄	270	0.73
49.	35.18	1(2H)-Naphthalenone, 3,4-dihydro-2-(1-naphthalenylmethylene)-	C ₂₁ H ₁₆ O	284	10.28
50.	35.36	Galangin	C ₁₅ H ₁₀ O ₅	270	2.15

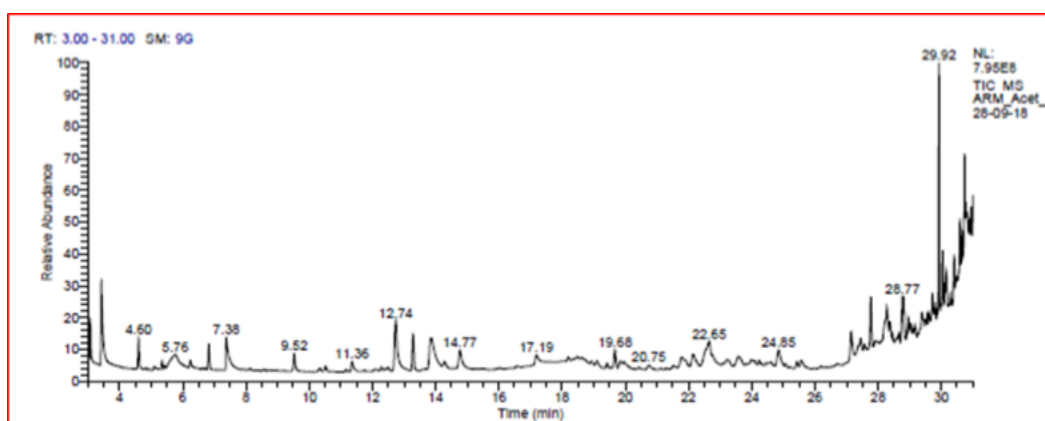


Figure 2 GC MS chromatogram of acetone extract of rhizome of *A. calcarata*

Table 3. Phytocompounds identified in the methanol extract of leaves of *A. calcarata*

Sl. No	RT	Name of compound	Molecular formula	MW	Peak area %
1.	3.12	2-Cyclopenten-1-one, 2-hydroxy-	C ₅ H ₆ O ₂	98	10.69
2.	3.75	Imidazole, 2-acetoxy-	C ₅ H ₆ N ₂ O ₂	126	0.37
3.	3.93	2H-Pyran-2,6(3H)-dione	C ₅ H ₄ O ₃	112	1.27
4.	5.66	4-Piperidinone, 2,2,6,6-tetramethyl-	C ₉ H ₁₇ NO	155	0.88
5.	6.60	Ethanone, 1-[4-(1-methyl-2-propenyl)phenyl]-	C ₁₂ H ₁₄ O		0.14
6.	7.57	Benzofuran, 2,3-dihydro-	C ₈ H ₈ O	120	3.41
7.	8.03	Naphthalene, 1,2,3,4-tetrahydro-1,1,6-trimethyl-	C ₁₃ H ₁₈	174	0.06
8.	9.14	2-Methoxy-4-vinylphenol	C ₉ H ₁₀ O ₂	150	9.57
9.	9.80	Phenol, 2,6-dimethoxy-	C ₈ H ₁₀ O ₃	154	0.50
10.	10.45	(+)-3-Carene, 10-(acetylmethyl)-	C ₁₃ H ₂₀ O	192	1.14
11.	11.77	Phenol, 2-methoxy-4-propyl-	C ₁₀ H ₁₄ O ₂	166	0.17
12.	12.12	4-(2,6,6-Trimethylcyclohexa-1,3-dienyl) but-3-en-2-one	C ₁₃ H ₁₈ O	190	0.62
13.	12.39	Stevioside	C ₃₈ H ₆₀ O ₁₈	804	0.28
14.	13.54	3,5-Dimethoxyacetophenone	C ₁₀ H ₁₂ O ₃	180	1.17
15.	13.60	3-Bromo-5,5-dimethyl-cyclohex-2-enol	C ₈ H ₁₃ BrO	204	0.75
16.	14.58	Megastigmatrienone	C ₁₃ H ₁₈ O	190	0.94
17.	15.18	Benzaldehyde, 4-hydroxy-3,5-dimethoxy-	C ₉ H ₁₀ O ₄		
18.	17.80	Isoquinoline, 1,2,3,4- tetrahydro- 6,7-dimethoxy-1,2-dimethyl-, (ñ)-	C ₁₃ H ₁₉ NO ₂	221	0.46
19.	17.89	Cinnamic acid, 4-hydroxy-3-methoxy-, methyl ester	C ₁₁ H ₁₂ O ₄	204	1.15
20.	18.92	Hexadecanoic acid, methyl ester	C ₁₇ H ₃₄ O ₂	270	1.12
21.	19.55	2-Pyrrolidinone, 1-(4-amino-3,5-dimethylphenyl)-	C ₁₂ H ₁₆ N ₂ O	204	0.38
22.	20.03	(E)-15,16-Dinorlabda-8(17),11-dien-13-one	C ₂₃ H ₃₄ O ₃	260	0.05
23.	20.10	trans-Sinapyl alcohol	C ₁₁ H ₁₄ O ₄	210	0.02
24.	23.67	Stigmast-5-en-3-ol, (3á,24S)-	C ₂₉ H ₅₀ O	414	1.01
25.	25.28	Ethyl isoallochololate	C ₂₆ H ₄₄ O ₅	436	2.78
26.	25.62	Milbemycin B	C ₃₃ H ₄₇ ClO ₇	590	2.63
27.	26.38	Cholestane-3,5-diol, 5-acetate, (3á,5à)-	C ₂₉ H ₅₀ O ₃	386	1.24
28.	26.89	Lupeol	C ₃₀ H ₅₀ O	426	1.84
29.	26.93	1-Heptatriacotanol	C ₃₇ H ₇₆ O	536	1.22
30.	27.95	Phytyldecanoate	C ₃₀ H ₅₈ O ₂	450	17.46
31.	28.90	5-Cholestene-3-ol, 24-methyl-	C ₂₈ H ₄₈ O	400	6.51
32.	29.13	Stigmast-4-en-3-one	C ₂₉ H ₄₈ O	412	1.80
33.	29.70	Stigmasterol	C ₂₉ H ₄₈ O	412	8.01

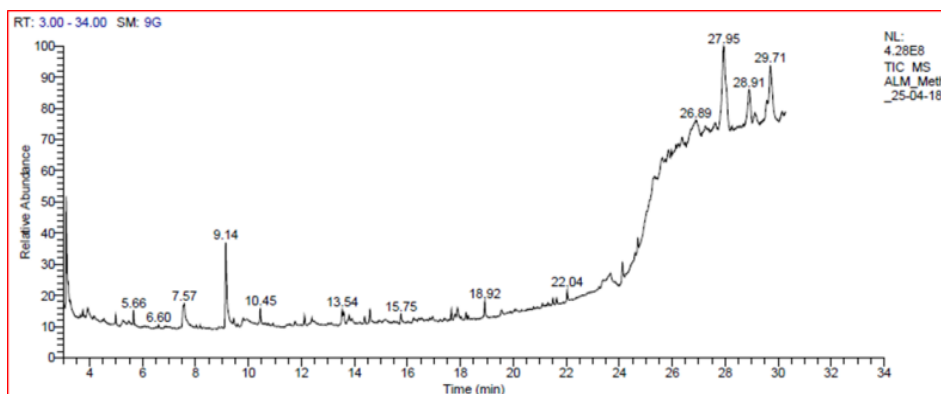


Figure 3. GC MS chromatogram of methanol extract of leaves of *A. calcarata*

8(17),11-dien-13-one has been reported from methanol and acetone extracts of the rhizome. It has been previously isolated and reported from rhizome [1]. (E)-15, 16-dinorlabda-8(17), 11-dien-13-one has been reported from the methanolic extract of leaves in this study for the first time. Also, the present study reports for the first time another dinorlabdanic diterpenoid compound (E)-15, 16-dinorlabda-8(17), 12-dien-14-al from the acetone extracts of rhizome. Acetone extract of rhizome contain compounds like naringenin, villosin, 6 epi shyobunol etc., which has not been previously reported from *A. calcarata*.

3.2/Total phenolic (TPC) and total flavonoid content (TFC)

In case of rhizome and leaves the highest TPC was found in acetone extract of leaves and highest TFC was found in the methanol extracts of leaves. The details of TPC and TFC are provided in table 4.

Table 4. TPC and TFC of *A. calcarata* rhizome and leaves

Name of the plant	Part	Extract	Total phenolic content (TPC)	Total flavonoid content (TFC)
<i>Alpinia calcarata</i>	Rhizome	Petroleum ether	26.59 ± 0.63	29.17 ± 1.39
		Acetone	124.6 ± 0.73	418.06 ± 0.80
		Methanol	115.95 ± 1.26	393.06 ± 2.12
		Aqueous	25.2 ± 2.03	15.30 ± 0.93
	Leaves	Petroleum ether	6.34 ± 0.50	59.72 ± 2.12
		Acetone	165.07 ± 0.73	362.5 ± 0.88
		Methanol	155.15 ± 1.26	427.77 ± 1.39
		Aqueous	10.2 ± 2.8	18.2 ± 0.09

Values are mean ± SD of three replicates. TPC milligram gallic acid equivalent /gm, TFC milligram rutin equivalent/gm

3.3/DPPH free radical scavenging activity

As per figures 4 & 5, in the DPPH scavenging assay, various extracts of rhizome and leaves of AC exhibited free radical scavenging activity by inhibiting DPPH[•] radical, which was dependent on concentrations of the extracts. The well-known antioxidant, ascorbic acid, showed high degree of free radical – scavenging activity than that of the plant extracts at each concentration points. The IC₅₀ of acetone extract of leaves were 201.37 ± 0.36 µg/ml and of methanol was 481.95 ± 0.35 µg/ml. For rhizome, acetone extracts showed IC₅₀ 250.61 ± 0.48 µg/ml and methanol extracts showed 357.27 ± 0.56 µg/ml.

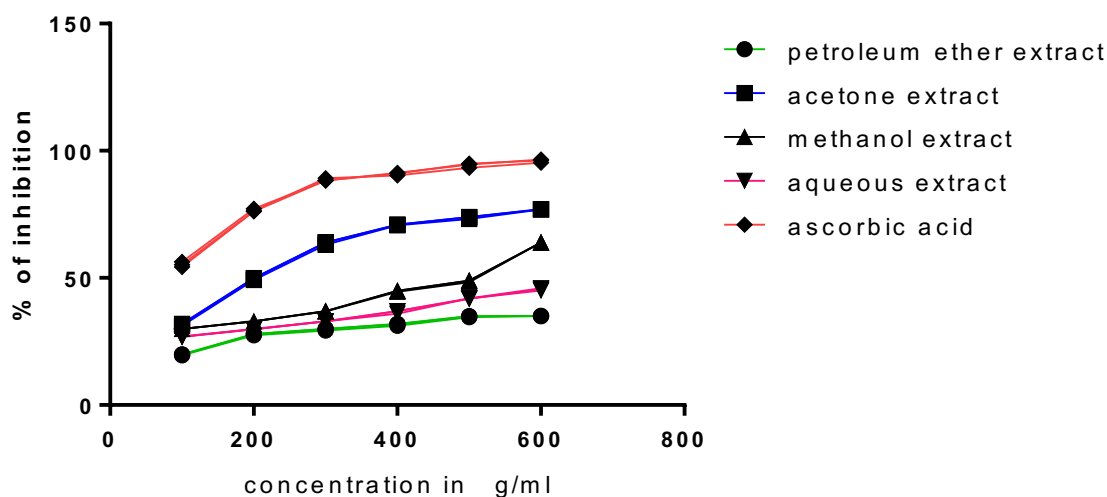


Figure 4. DPPH radical scavenging activity of various extracts of leaves of *A. calcarata* along with the standard ascorbic acid. (Mean \pm SD, n= 3). Concentration in $\mu\text{g/ ml}$.

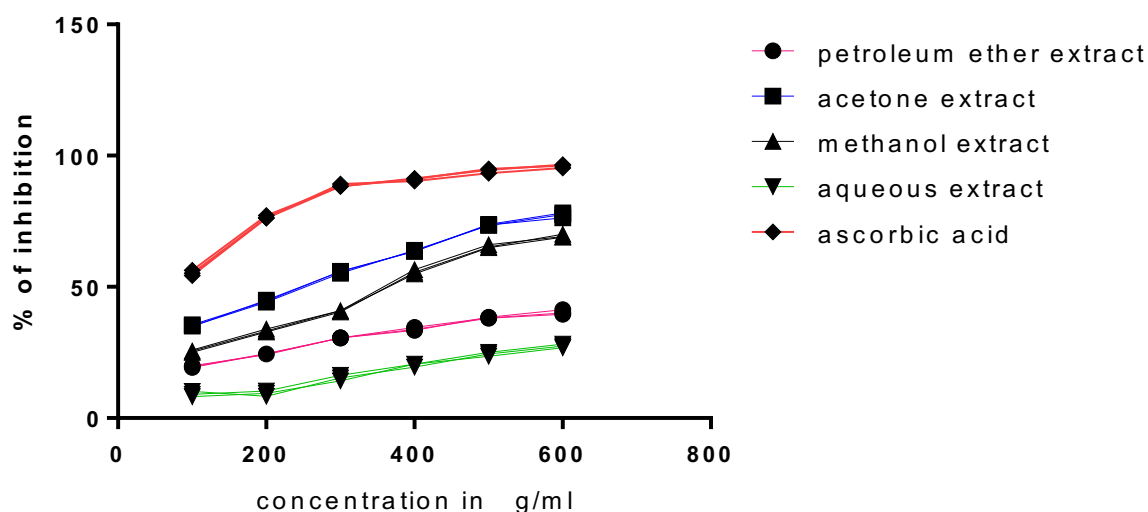


Figure 5 DPPH radical scavenging activity of various extracts of rhizome of *A. calcarata* along with the standard ascorbic acid. (Mean \pm SD, n= 3). Concentration in $\mu\text{g/ ml}$.

Among the studied extracts of *A. calcarata*, acetone extracts of leaves and rhizome showed high radical scavenging activity and moreover leaf extracts are more active than rhizome extracts based on IC_{50} . It has been identified by Ramya *et al.*, [8] that *A. calcarata* rhizome ethanolic extracts has significant amount of phenolics and flavonoids and shows good antioxidant properties from Tamilnadu. Tripathi & Swain [14] reported high in vitro antioxidant activity and free radical scavenging property for the cold ethanolic extracts of rhizomes of *A. calcarata* from Andaman islands. Hema [1] reported from South Kerala that high phenolic and flavonoid content was present in the acetone extract of rhizome of *A. calcarata* and it shows high antioxidant activity than ethanolic extracts of rhizome. In the present study also acetone extracts of rhizome showed high antioxidant activity, phenolic and flavonoid content, than other extracts showing close similarity with the study conducted by Hema [1]. The difference in the results of the study conducted by Ramya *et al.*, [8] and Tripathi & Swain [14] with Hema [1] and the present study may be different growth period, geographic location, genetic diversity etc. of *A. calcarata* as explained by Tripathi & Swain [14] in their study at Andaman islands.

3.4 /Reducing power assay

Figures 6 & 7 shows the reducing power capabilities of the plant extracts compared to ascorbic acid. The various extracts of leaves and rhizome of *A. calcarata* displayed good reducing power and was found to rise with increasing concentrations of the extract. Among the extracts, acetone extract showed maximum reducing power both in the case of leaves and rhizomes.

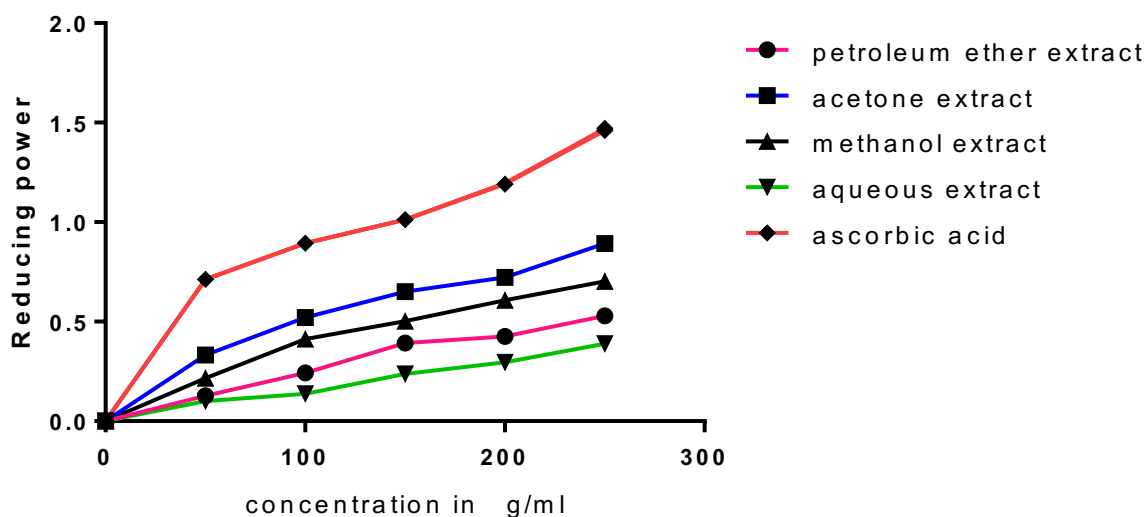


Figure 6. Reducing power of various extracts of leaves of *A. calcarata* along with ascorbic acid. (Mean \pm SD, n= 3).

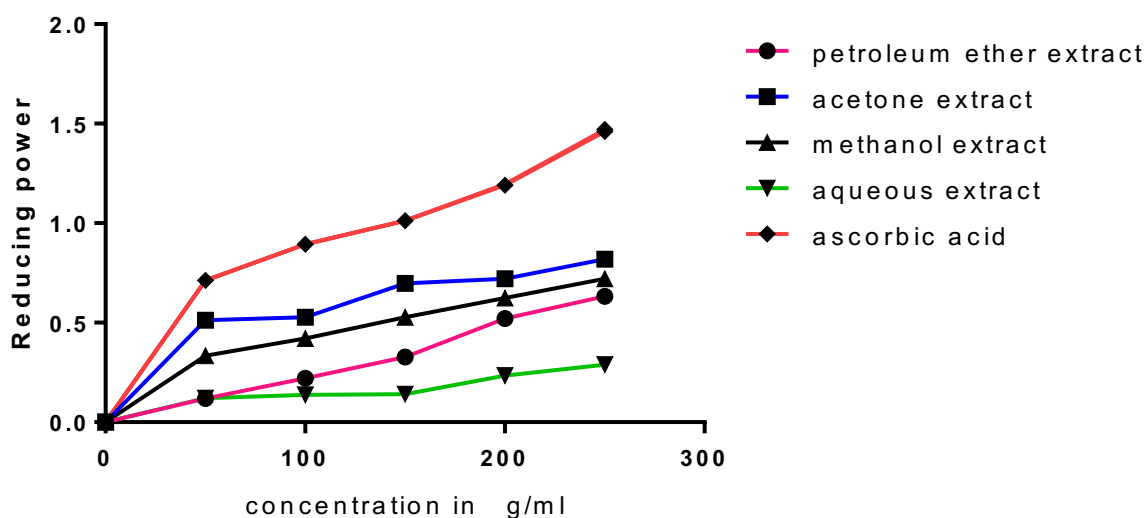


Figure 7. Reducing power of various extracts of rhizome of *A. calcarata* along with ascorbic acid. (Mean \pm SD, n= 3).

3.5/Total antioxidant capacity (Phosphomolybdenum assay)

The total antioxidant capacities of the leaf and rhizome extracts of *A. calcarata* are given in table 5. It can be identified that acetone extracts of leaves and rhizome shows high total antioxidant capacity and it can be correlated with DPPH and reducing power assay. All the antioxidant assays prove that acetone extracts are showing high radical scavenging activity and leaf extracts are more active than

rhizome extracts of *A. calcarata*. The antioxidant activity and total phenolic and flavonoid content of rhizome of *A. calcarata* show close resemblance with studies reported by Hema [1]. As per our knowledge this is the first study reporting antioxidant activities of leaf extracts of *A. calcarata*.

Table 5. Total antioxidant capacity of rhizome and leaf extracts of *A. calcarata*

Name of the plant	Part	Extract	Total antioxidant capacity equivalent to ascorbic acid mg/gm plant extract
<i>Alpinia calcarata</i>	Rhizome	Petroleum ether	42.40 ± 1.67
		Acetone	248.2 ± 1.52
		Methanol	152.4 ± 2.20
		Aqueous	14.20 ± 1.08
	Leaves	Petroleum ether	56.39 ± 1.27
		Acetone	302.00 ± 1.67
		Methanol	252.06 ± 1.27
		Aqueous	11.38 ± 0.83

3.6 /Correlation analysis

In order to find the correlation between TPC & TFC with antioxidant activity of selected plants, pearson correlation analysis (r value) was performed and results are tabulated in table 6. Strong positive correlations were obtained between TPC and TFC of *A.calcarata* extracts and antioxidant activity by DPPH and phosphomolybdenum method while reducing power method showed good correlation with TPC of *A.calcarata* leaves only (r = 0.91) .

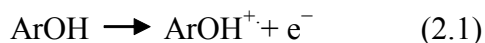
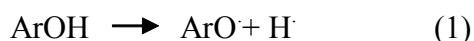
Table 6. Pearson correlation coefficient (r) values for correlation between TPC /TFC of *A.calcarata* leaves and rhizome extracts

Plant extract	TPC / TFC	DPPH	Phosphomolybdenum method	Reducing power
<i>A.calcarata</i> leaves	TPC	0.919*	0.985*	0.91*
<i>A.calcarata</i> rhizome	TPC	0.975*	0.972*	0.791
<i>A.calcarata</i> leaves	TFC	0.938*	0.962*	0.863
<i>A.calcarata</i> rhizome	TFC	0.976*	0.968*	0.798

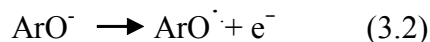
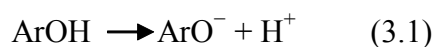
*Significant correlation at p < 0.05 levels TPC – Total phenolic content expressed as mg/g Gallic acid equivalents
TFC – Total flavonoid content expressed as mg/g Rutin equivalents

3.7 /Theoretical studies on antioxidant activity

Antioxidants prevent destructive free radical chain reactions by scavenging them through electron transfer mechanisms. It has been identified that antioxidant activity of phenolic compounds including flavonoids depend upon their structural characteristics and their ability to donate protons and electrons to prevent the energetic oxidising agents including free radicals. Electronic interactions of phenolic compounds within the cell explain the biological activity of these compounds. To understand the mechanism of antioxidant activity of the compounds, study of molecular and electronic properties is important. Phenolic compounds scavenge free radicals by the following methods. There are two accepted mechanisms of phenolic antioxidants, hydrogen atom transfer (HAT) and single electron transfer followed by proton transfer (SET – PT).



A recently discovered mechanism – sequential proton loss electron transfer (SPLET) mechanism is as:



Though the net result of the three mechanisms are same (formation of phenoxy radical) from antioxidant action view point, under certain conditions one of the possible mechanisms may prevail. The reaction enthalpies related to the three antioxidant mechanisms are calculated using DFT/B3LYP method and they are denoted as follows:

BDE – bond dissociation enthalpy related to equation 1

IP_r – ionization potential, enthalpy of electron transfer from the antioxidant molecule, Eq. (2.1)

PDE – proton dissociation enthalpy, Eq. (2.2)

PA – proton affinity of phenoxide ion, Eq. (3.1)

ETE – electron transfer enthalpy, Eq. (3.2).

In the present study DFT studies of selected phenolic compounds including flavonoids from *A. calcarata* rhizome and leaves were conducted. All calculations were performed with the Gaussian 09 program package using density functional theory (Frisch *et al.*) [25]. The geometry of each compound, radical, radical cation and anion was optimized using DFT (density functional theory) method with UB3LYP functional. The calculations were performed in 6-311G (d,p) basis set (Binkley *et al.*) [26]. Obtained total energy of the hydrogen atom, $-0.499897 E_h$, was used in the BDE calculations. In the case of DFT method, which does not provide enthalpies directly, the total enthalpies of the species X, $H(X)$, at temperature T are usually estimated from the expression :

$$H(X) = E_0 + ZPE + \Delta H_{\text{trans}} + \Delta H_{\text{rot}} + \Delta H_{\text{vib}} + RT \quad (5)$$

where E_0 is the calculated total electronic energy, ZPE stands for zero-point energy, ΔH_{trans} , ΔH_{rot} , and ΔH_{vib} are the translational, rotational and vibrational contributions to the enthalpy. Finally, RT represents PV-work term and is added to convert the energy to enthalpy. ΔH_{trans} ($3/2RT$), ΔH_{rot} ($3/2RT$ or RT for a linear molecule), and ΔH_{vib} contributions to the enthalpy are calculated from standard formulas:

$$\text{BDE} = H(\text{ArO}^\cdot) + H(\text{H}^\cdot) - H(\text{ArOH}) \quad (5)$$

$$\text{IP}_r = H(\text{ArOH}^{+\cdot}) + H(\text{e}^-) - H(\text{ArOH}) \quad (6)$$

$$\text{PDE} = H(\text{ArO}^\cdot) + H(\text{H}^+) - H(\text{ArOH}^{+\cdot}) \quad (7)$$

$$\text{PA} = H(\text{ArO}^-) + H(\text{H}^+) - H(\text{ArOH}) \quad (8)$$

$$\text{ETE} = H(\text{ArO}^\cdot) + H(\text{e}^-) - H(\text{ArO}^-) \quad (9)$$

The calculated enthalpy of proton, $H(\text{H}^+)$, is $6.197 \text{ kJ mol}^{-1}$; the enthalpy of electron, $H(\text{e}^-)$, is $3.145 \text{ kJ mol}^{-1}$ (Bartmess) [27]. All reaction enthalpies defined in Eqs. (5) – (9) were calculated for 300 K. Quantum chemical parameters such as the energies of frontier molecular orbitals, (E_{HOMO}) and (E_{LUMO}), the separation energy ($E_{\text{HOMO}} - E_{\text{LUMO}}$ ie ΔE), representing the function of reactivity, electronegativity (χ), global softness (σ), global hardness (η) etc. are also calculated using the following equations, where I (Ionisation potential), electron affinity (A) which are defined as $I = -E_{\text{HOMO}}$ and $A = -E_{\text{LUMO}}$

$$\chi = \frac{I+A}{2} \quad (10)$$

$$\eta = \frac{I-A}{2} \quad (11)$$

$$\sigma = 1/\eta = -2/ E_{\text{HOMO}} - E_{\text{LUMO}} \quad (12)$$

Quantum chemical parameters like energies of frontier molecular orbitals, (E_{HOMO}) and (E_{LUMO}), the separation energy ($E_{\text{HOMO}} - E_{\text{LUMO}}$) (ΔE), representing the function of reactivity, electronegativity (χ), global softness (σ), global hardness (η) etc. are important in determining the reactivity and stability of molecules. Hardness indicates the ability to resist the release of electrons. Global softness is the capacity of an atom or group of atoms to receive electrons. Thus, a low value of hardness and high value of softness indicate good reactivity. The quantum chemical parameters calculated for selected phenolic compounds including flavonoids are represented in table 7. In the present study the three mechanisms responsible for antioxidant activity of compounds *viz.*, HAT, SET -PT and SPLET are explored by DFT methods. Hence parameters such as BDE, IP, PDE, PA and ETE were determined. The calculated values of BDE in gas phase are presented in table 8. Low value of BDE indicates the ease of O-H bond dissociation and hence the ability to show better antioxidant activity by HAT mechanism.

Table 7. Quantum chemical parameters of different components of *A. calcarata*

Sl No.	Name of the compound	HOMO (eV)	LUMO (eV)	HOMO - LUMO (eV)	χ (electronegativity) (eV)	η (global hardness) (eV)	σ (global softness) (eV)
1	Phenol, 2,6-dimethoxy-	-5.79	0.12	5.9	2.84	2.95	0.34
2	2-Methoxy-4-vinylphenol	-5.55	-0.84	4.71	3.2	2.35	0.42
3	Cinnamic acid, 4-hydroxy-3-methoxy-, methyl ester	-6.05	-1.72	4.33	3.88	2.17	0.46
4	4-(1-Hydroxyallyl)-2-methoxyphenol	-5.91	-0.39	5.51	3.14	2.75	0.36
5	5,7 dihydroxy flavanone [Galangin]	-5.79	-1.87	3.92	3.83	1.96	0.51
6	4H-1-Benzopyran-4-one, 2,3-dihydro-5,7-dihydroxy-2-phenyl-, (S)- [Dihydrochrysin]	-6.34	-1.3	5.04	3.82	2.52	0.4
7	4H-1-Benzopyran-4-one, 2,3-dihydro-5,7-dihydroxy-2-(4-hydroxyphenyl)-, (S)- [Naringenin]	-6.07	-1.63	4.44	3.85	2.22	0.45

Table 8 clearly indicates that the energies for O-H bond dissociation of the studied components are comparable with that of the standard antioxidant compounds except for a few. The BDE values of phenol, ascorbic acid and trolox taken as standards were respectively 83.50 Kcal/mol, 73.9 Kcal/mol and 73 Kcal/mol. It can be identified from the table 8 that 4-(1-Hydroxyallyl)-2-methoxyphenol have very low value of O - H BDE, indicating high antioxidant efficacy. The values of ionization potential (IP) and proton dissociation enthalpy (PDE) which explains the SET - PT mechanism of antioxidant activity are also provided in table 8. The IP value indicates the electron donating capacity of the molecule in the first step of the mechanism. Lower the IP value easier to donate the electrons and consequently higher will be the antioxidant capacity. It can be identified from the table that all the selected compounds from the plants exhibited low IP values compared with standards phenol (192.3 Kcal/mol) and ascorbic acid (193.9 Kcal/mol). Compound 5,7 dihydroxy flavanone (Galangin) showed very low IP value (165.63 Kcal/mol) . The last step in the SET –PT mechanism involves a proton loss from the radical

cation formed in the first step, which is governed by proton dissociation enthalpy. Lower the PDE value greater is the antioxidant activity. It can be identified from table 8 that 2,6 dimethoxy phenol has lowest PDE value (213.60 Kcal/mol) comparable with standards phenol (207.2 Kcal/mol) and ascorbic acid (229.8 Kcal/mol). No compound showed PDE value less than standard trolox (196 Kcal/mol). The antioxidant activity by SET –PT mechanism can be explained by the combination of IP and PDE [28]. This is provided in table 8 from which it is clear that all the selected phytochemicals possess good antioxidant potential when compared to the standards. The compound 5, 7 dihydroxy flavanone show highest antioxidant potential followed by 4H-1-Benzopyran-4-one, 2,3-dihydro-5,7-dihydroxy-2-(4-hydroxyphenyl)-, (S)- or (Naringenin) than other studied compounds. The proton affinity (PA) and electron transfer enthalpy (ETE) values of different components analysed are given in table 8.

The first step in the SPLET mechanism is governed by PA as this step involves the loss of a proton to form phenoxide anion. Thus, low value of PA indicates good antioxidant activity of the compound. It can be identified from the table that the proton affinities of the selected compounds are very low and are almost equal to that of the standards. 5,7-dihydroxy flavanone (Galangin) has the lowest PA value (331.42 Kcal/mol) and 2,6 dimethoxy phenol have the highest PA value (353.99 Kcal/mol).

Table 8. Thermochemical parameters of *A. calcarata*

Sl No.	Name of the compound	BDE (Kcal/mol)	IP (Kcal/mol)	PDE (Kcal/mol)	IP + PDE (Kcal/mol)	PA (Kcal/mol)	ETE (Kcal/mol)	PA + ETE (Kcal/mol)
1	Phenol, 2,6-dimethoxy-	76.68	175.21	213.6	388.81	353.99	38.56	392.55
2	2-Methoxy-4-vinylphenol	79.1	166.71	228.26	394.97	350.7	44.27	394.97
3	Cinnamic acid, 4-hydroxy-3-methoxy-, methyl ester	78.61	175.5	218.98	394.46	333.06	61.42	394.48
4	4-(1-Hydroxyallyl)-2-methoxyphenol	74.17	167.99	222.04	390.03	345.5	44.54	390.04
5	5,7 dihydroxy flavanone [Galangin]	82.39	165.63	232.62	398.25	331.42	66.82	398.24
6	4H-1-Benzopyran-4-one, 2,3-dihydro-5,7-dihydroxy-2-phenyl-, (S)- [Dihydrochrysin]	90.68	180.12	226.43	406.54	337.43	69.11	406.54
7	4H-1-Benzopyran-4-one, 2,3-dihydro-5,7-dihydroxy-2-(4-hydroxyphenyl)-, (S)- [Naringenin]	81.6	171.11	226.36	397.46	333.71	63.75	397.46
8	Phenol	83.5	192.3	207.2	399.5	347.8	51.6	399.4
9	Ascorbic acid	73.9	193.9	229.8	423.7	325.9	63.9	389.8
10	Trolox	73	159.1	196	355.1	347.1	41.9	389

The last step in the SPLET mechanism is controlled by ETE, since it involves an electron transfer process. Low value of ETE is a good indicator of antioxidant potential. It can be identified from the table that the ETE of phenol 2, 6 dimethoxy (38.56 K Cal/mol) is lower than that of the standard. As described previously, the SPLET mechanism can be effectively explained by the combination of PA and ETE. It can be identified from table 8 that on comparison with the standard, the compound 4 -(1- Hydroxyallyl)-2-methoxyphenol showed best antioxidant potential of 390.04 Kcal/mol. Other studied compounds also showed good antioxidant potential as observed from the obtained data. Different antioxidant assays are based on different mechanisms of action. DPPH radical scavenging method of analysis is considered to take place via both HAT and SET - PT mechanism while reducing power assays proceed via SET – PT mechanism [29]. It is generally believed that the three mechanisms of antioxidant action may co-exist

together or one of the mechanisms may prevail under certain conditions. The solvents also have marked effect on the mechanism of antioxidant activity. In order to better understand the mechanism of antioxidant activities, atomic spin densities (ASD), natural bond population charge (NBP) and singly occupied molecular orbitals (SOMO) of the transition states of the molecules should be determined and studied.

3.8/ Corrosion inhibition studies

Methanolic extracts of rhizome and leaves of AC has been studied for corrosion inhibitory potential against mild steel in 1 M HCl by weight loss method, FT-IR and SEM. Adsorption studies has also been carried out. Theoretical studies of four major compounds from the leaves viz., Cinnamic acid, 4-hydroxy-3-methoxy, methylester, 4-Piperidinone, 2,2,6,6-tetramethyl, Stigmasterol and 4-(2,6,6-Trimethylcyclohexa-1,3-dienyl) but-3-en-2-one and five major compounds from rhizome of *A. calcarata*, viz., Benzene 1,3 dimethoxy-5-(1E)-2-Phenylethenyl, 2,6 dimethoxy phenol, 7 methoxy coumarin and Calcaratarin C has been carried out.

3.9/ Weight loss method

The corrosion rate and inhibition efficiencies were done following standard procedures (Bribri *et al.*) [30] with the following equations:

$$\text{Corrosion rate (C}_R\text{)} = (W_b - W_a) / A \times t \quad (13)$$

$$\text{Inhibition efficiency (IE \%)} = [(W_1 - W_2) / W_1] \times 100 \quad (14)$$

where W_a and W_b are the weight of steel specimens after and before immersions in the corrosion media, A the area of steel specimen in cm^2 , t the time of exposure in hours, W_1 the weight loss without inhibitor and W_2 the weight loss with inhibitor. The weight loss measurement results conducted at 303 K, 313K and 323 K for leaf and rhizome extracts are provided in tables 9 & 10. It can be noted that with increasing inhibitor concentration the inhibition efficiency percentage increased. But IE % decreases with increase in temperature. AC rhizome extract showed maximum inhibition efficiency of 92 % than leaf extracts which showed only 90.10 % IE at 303 K.

3.10/ Adsorption studies and thermodynamic parameters

Metal – inhibitor interaction is due to adsorption of an organic molecule on the metal surface, which is a replacement reaction and it can be well studied by analyzing the adsorption process using adsorption isotherms [31]. It provides information regarding the interaction between inhibitor and mild steel surface. The frequently used adsorption isotherms are Temkin, Frumkin and Langmuir isotherms. The experimental data was tested on these adsorption isotherms and through correlation coefficient (R^2) usage the best fit was obtained from Langmuir adsorption isotherm. The surface interaction of *A. calcarata* leaf and rhizome extracts on mild steel in 1 M HCl was obeying Langmuir adsorption isotherm at all temperatures (303K, 313K and 323K). Langmuir adsorption isotherm is described by the equation :

$$C_{inh} / \theta = 1/K_{ads} + C_{inh} \quad (15)$$

where C_{inh} represent the concentration of the inhibitor, K_{ads} is the equilibrium constant of adsorption process and θ the surface coverage. Figures 8 & 9 represent the Langmuir adsorption isotherms of selected plants which are found to be linear. In the present study the value of correlation coefficient (R^2) was obtained close to unity for Langmuir adsorption isotherm.

Table 9. Corrosion parameters of mild steel in the absence and presence of *A.calcarata* leaf extract

Temperature	Concentration of plant extract in 1M HCl (ppm)	Weight of steel before immersion	Weight of steel after immersion	Weight loss	Corrosion rate (CR in g/cm ² h)	Inhibition efficiency (IE %)
303K	Blank	3.257	3.1849	0.0721	3.16	
	100	3.257	3.231	0.026	1.14	63.9
	150	3.651	3.6297	0.0213	0.93	70.5
	200	3.254	3.2366	0.0174	0.77	75.8
	250	3.253	3.241	0.012	0.52	83.4
	300	3.158	3.1509	0.0071	0.31	90.1
313K	Blank	3.784	3.6693	0.1147	5.03	
	100	3.654	3.6097	0.0443	1.94	61.4
	150	3.251	3.2144	0.0366	1.6	68.1
	200	3.294	3.2633	0.0307	1.35	73.2
	250	3.547	3.5257	0.0213	0.94	81.4
	300	3.215	3.2014	0.0136	0.6	88.1
323K	Blank	3.741	3.5982	0.1428	6.26	
	100	3.652	3.5938	0.0583	2.56	59.2
	150	3.298	3.25	0.048	2.1	66.4
	200	3.258	3.2172	0.0408	1.79	71.4
	250	3.264	3.2343	0.0297	1.3	79.2
	300	3.267	3.2474	0.0196	0.86	86.3

Table 10. Corrosion parameters of mild steel in the absence and presence of *A.calcarata* rhizome extract

Temperature	Concentration of plant extract in 1M HCl (ppm)	Weight of steel before immersion	Weight of steel after immersion	Weight loss	Corrosion rate (CR in g/cm ² h)	Inhibition efficiency (IE %)
303 K	Blank	3.061	2.9401	0.0763	3.35	
	100	3.754	3.735	0.0189	0.83	75.2
	150	3.728	3.7131	0.0148	0.65	80.5
	200	3.664	3.6517	0.0122	0.54	84
	250	3.748	3.7388	0.0091	0.4	88
	300	3.742	3.7358	0.0061	0.27	92
313 K	Blank	3.063	2.9532	0.1102	4.84	
	100	3.754	3.7233	0.0306	1.34	72.2
	150	3.728	3.7035	0.0245	1.07	77.8
	200	3.664	3.6438	0.0201	0.88	81.7
	250	3.712	3.6956	0.0163	0.72	85.2
	300	3.687	3.6753	0.0116	0.51	89.4
323K	Blank	3.726	3.5847	0.1417	6.22	
	100	3.754	3.7103	0.0436	1.91	69.2
	150	3.728	3.6922	0.0359	1.57	74.7
	200	3.664	3.6332	0.0307	1.35	78.3
	250	3.712	3.6864	0.0255	1.12	82
	300	3.654	3.6341	0.0198	0.87	86

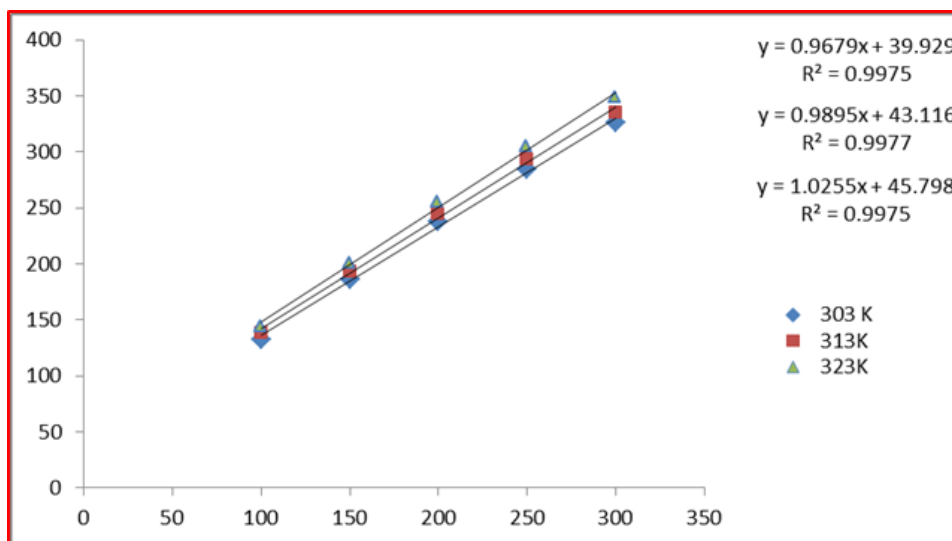


Figure 8. Langmuir adsorption isotherm of rhizome of *A. calcarata*

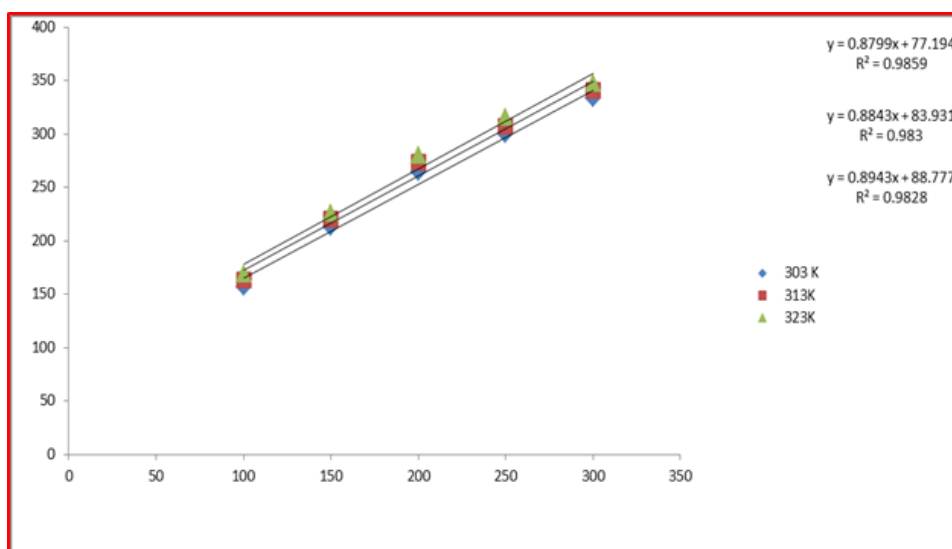


Figure 9. Langmuir adsorption isotherm of leaves of *A. calcarata*

3.11/ Theoretical calculations

Quantum chemical studies are an excellent tool in determining the molecular structure, electronic structure as well as reactivity of molecules in corrosion studies [32]. Certain quantum chemical calculations were performed to study the effect of molecular structure on inhibition efficiency using Gaussian 09 programme package.

Certain major compounds from the selected plants were identified and theoretically studied. Quantum chemical parameters obtained from the calculations such as the energies of frontier molecular orbitals (E_{HOMO}) and (E_{LUMO}), the separation energy ($E_{\text{HOMO}} - E_{\text{LUMO}}$) (ΔE), representing the function of reactivity, electronegativity (χ), electron affinity (EA), global softness (σ), global hardness (η), ionization energy (IE), ΔN representing the fraction of electrons transferred from ligand to metal are collected in tables 11 -12. Electronegativity (χ), chemical hardness (η), global chemical softness (capacity of an atom or group of atoms to receive electrons) and number of transferred electrons (ΔN) were calculated using the following equations 16 -19. E is the ionization potential and A is electron affinity and $E = -E_{\text{HOMO}}$ and $A = -E_{\text{LUMO}}$

$$\chi = \frac{E+A}{2} \quad (16)$$

$$\eta = \frac{E-A}{2} \quad (17)$$

$$\sigma = 1/\eta = -2/ E_{\text{HOMO}} - E_{\text{LUMO}} \quad (18)$$

$$\Delta N = \chi_{\text{Fe}} - \chi_{\text{inh}} / 2 (\eta_{\text{Fe}} + \eta_{\text{inh}}) \quad (19)$$

Electronic structures of some of the major phytochemicals selected in the study are illustrated in Figures 10 - 13, which include optimized geometry, the highest occupied molecular orbital (HOMO) and lowest unoccupied molecular orbital (LUMO). E_{HOMO} show the electron donating ability of molecules and generally the higher the E_{HOMO} value, the greater the tendency of the molecule to donate electrons to acceptor molecule and the lower the E_{LUMO} value (electron accepting ability of the molecule) the greater the tendency to accept electrons [33,34]. The energy difference between E_{HOMO} and E_{LUMO} , ΔE , indicate the reactivity (inhibition efficiency) of the given compound and generally smaller the ΔE value, the greater will be the efficiency of the molecule [33,35]. The ionisation energy (IE) and electron affinity (EA) is related to E_{HOMO} and E_{LUMO} as per below [36,37]. (Ramya & Joseph 2015, Lukovits *et al.*, 2001).

$$I = - E_{\text{HOMO}} \quad (20)$$

$$A = - E_{\text{LUMO}} \quad (21)$$

The lower value of ΔE will render good inhibition efficiencies, since the energy to remove an electron from the last occupied orbital will be minimised. In the present study the obtained ΔE values are also very low values. The fraction of the electrons transferred from the inhibitor molecule to the metal surface i.e. ΔN , is less than 3.6, the efficiency of inhibition increases with increasing electron donating ability of the inhibitor to the metal surface. In the present study the phytochemicals studied have ΔN value less than 3.6 indicating high corrosion inhibition efficiency.

Table 11. Quantum chemical parameters of phytochemicals of *A. calcarata* leaves

Chemical constituent	HOMO (eV)	LUMO (eV)	ΔE (eV)	IE	EA	χ (electron gativity) (eV)	η (global hardness) (eV)	σ (global softness) (eV)	ΔN (eV)
Cinnamic acid, 4-hydroxy-3-methoxy, methyl ester	-6.05	-1.72	4.33	6.05	1.72	3.88	2.17	0.46	0.72
4- Piperidinone, 2,2,6,6-tetramethyl-	-6.37	-1.09	5.28	6.37	1.09	3.73	2.64	0.38	0.62
Stigmasterol	-6.31	0.36	6.67	6.31	-0.36	2.98	3.34	0.3	0.6
4-(2,6,6-Trimethyl cyclohexa-1,3 -dienyl) but-3-en-2-one	-6.78	-1.49	5.29	6.78	1.49	4.13	2.64	0.38	0.54

Table 12. Quantum chemical parameters of phytochemicals of *A. calcarata* rhizome

Chemical constituent	HOMO (eV)	LUMO (eV)	ΔE (eV)	IE	EA	χ (electron gativity) (eV)	η (global hardness) (eV)	σ (global softness) (eV)	ΔN (eV)
7methoxycoumarin	-6.32	-1.9	4.42	6.32	1.9	4.11	2.21	0.45	0.65
Calcaratarin C	-6.96	-1.11	5.85	6.96	1.11	4.04	2.92	0.34	0.51
Benzene, 1,3-dimethoxy-5-(1E)-2-Phenylethenyl	-5.64	-1.56	4.078	5.64	1.56	3.6	2.04	0.49	0.83
Phenol, 2,6-dimethoxy	-5.79	0.12	5.9	5.79	-0.12	2.84	2.95	0.34	0.71
4-hydroxyallyl-2 methoxy phenol	-5.91	-0.39	5.51	5.91	0.39	3.15	2.76	0.36	0.7

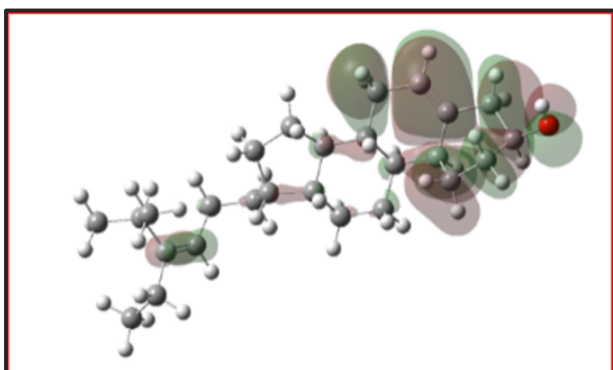


Fig: 10 a. HOMO Stigmasterol

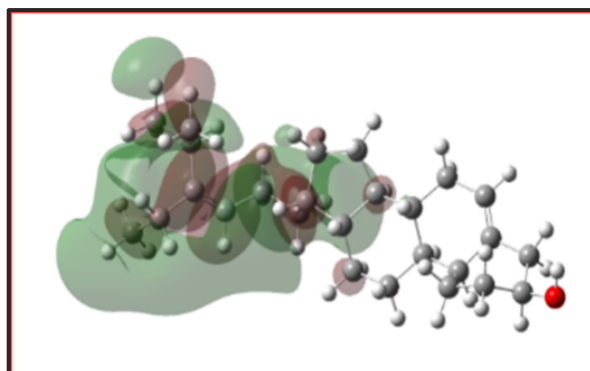


Fig: 10 b. LUMO Stigmasterol

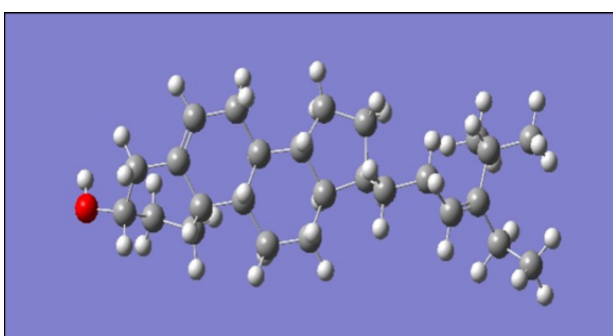


Fig: 10 c. Optimised geometry of Stigmasterol

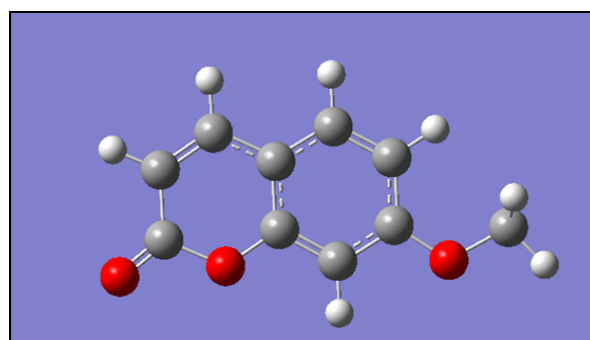


Fig: 11a. Optimised geometry of 7 methoxy coumarin

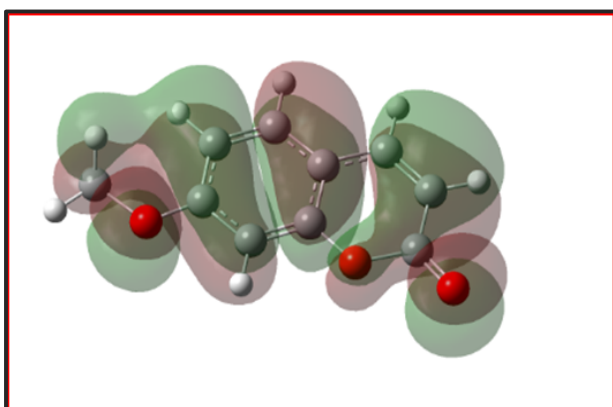


Fig: 11b. HOMO 7 methoxy coumarin

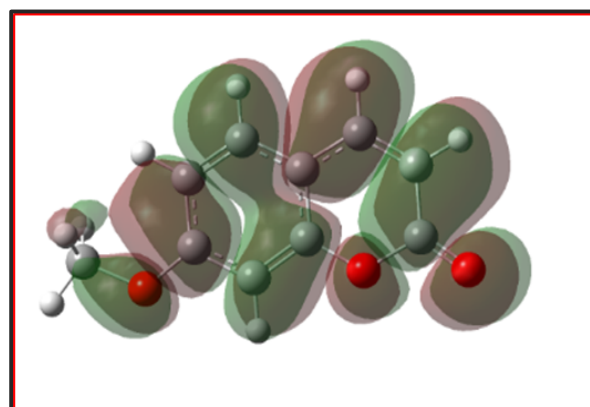


Fig: 11 c. LUMO 7 methoxy coumarin

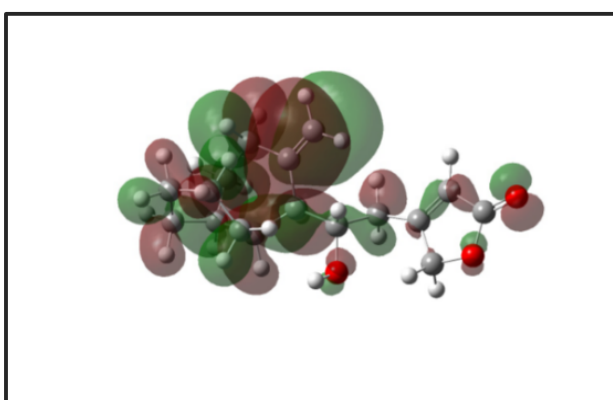


Fig : 12a. HOMO Calcaratarin C

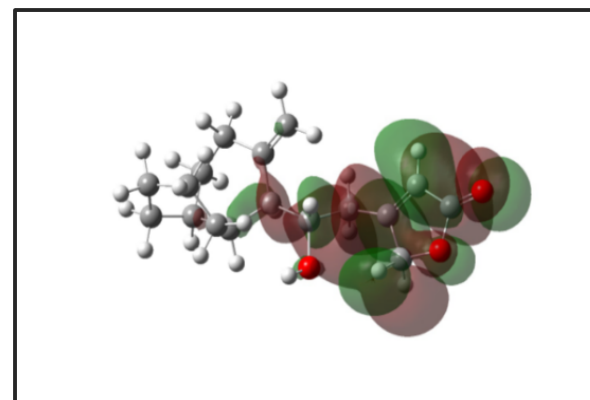


Fig: 12 b. HOMO Calcaratarin C

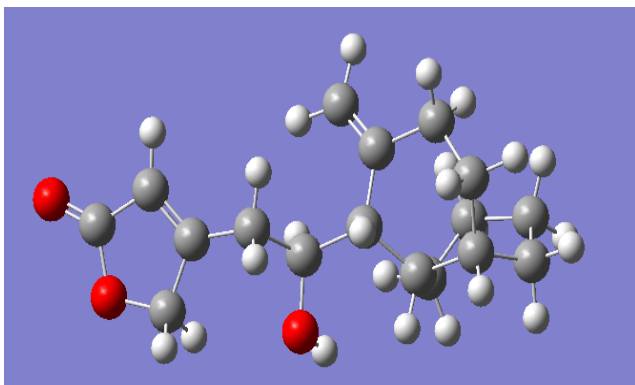


Fig :12c. Optimised geometry of Calcaratarin C

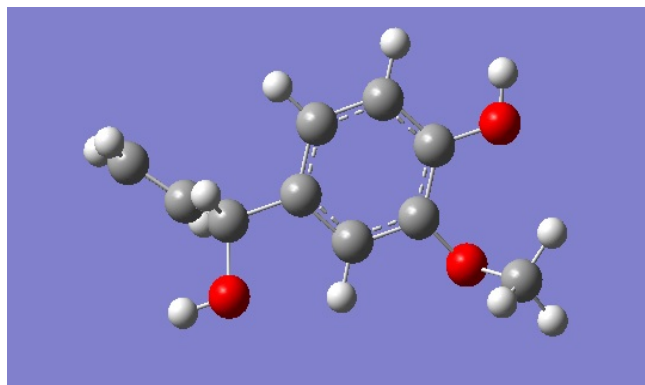


Fig:13a. Optimised geometry of 4Hydroxyallyl 2 methoxyphenol

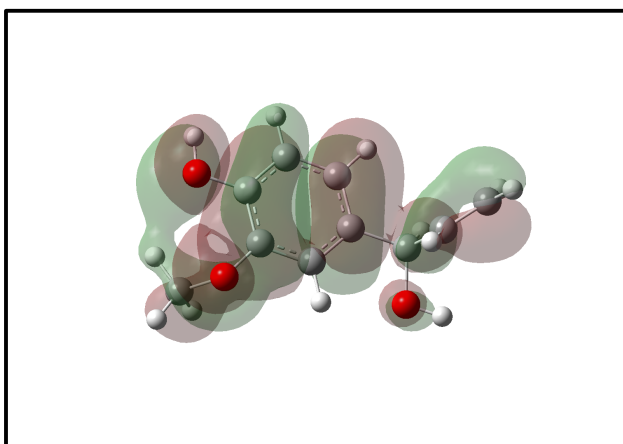


Fig:13 b. HOMO 4 Hydroxyallyl-2-methoxyphenol

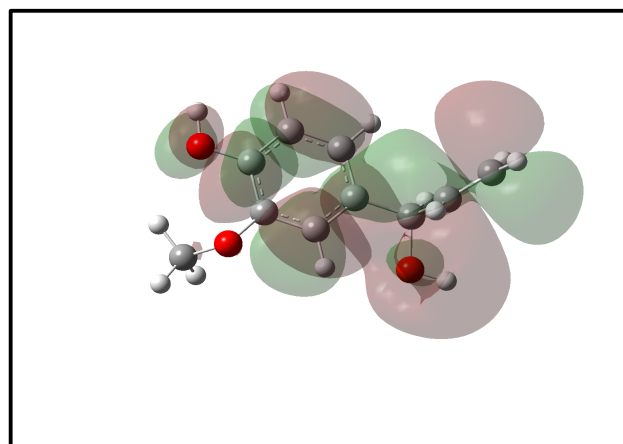


Fig:13c. LUMO 4 Hydroxyallyl-2-methoxyphenol

3.12 /Scanning electron microscopic studies (SEM)

SEM studies were conducted to study the surface morphology of mild steel before and after immersion in 1M HCl without and with *A.calcarata* rhizome and leaf extracts (300 ppm) and the results obtained are provided in [figures 15,16 and 17](#). From the figures it is clear that the extract form a protective film over mild steel specimens and prevent corrosion by acid solutions.

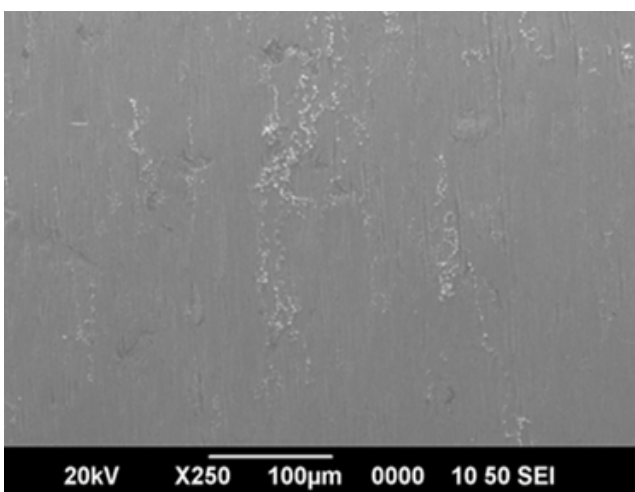


Fig: 14. SEM image of polished mild steel before immersion in test solution

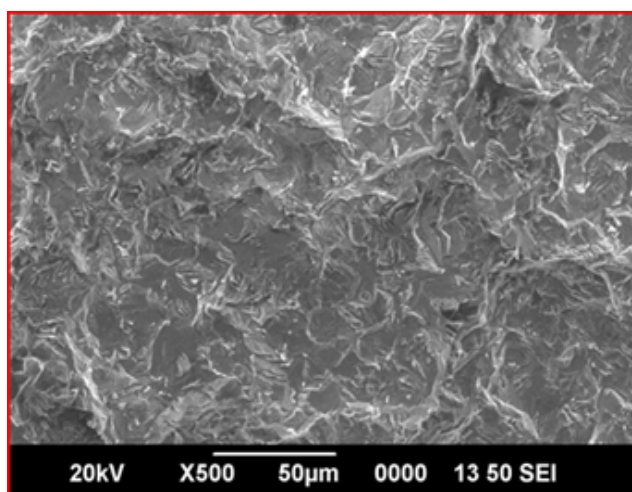


Fig: 15. SEM image of mild steel after immersion in 1M HCl without inhibitor

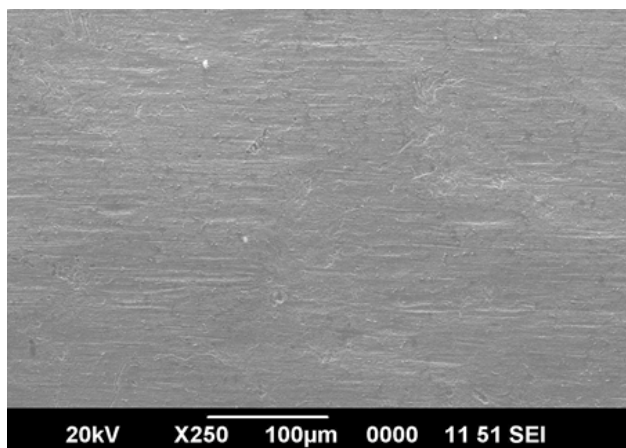


Fig:16. SEM image of mild steel after immersion in 1M HCl with *A.calcarata* leaf extract 300ppm

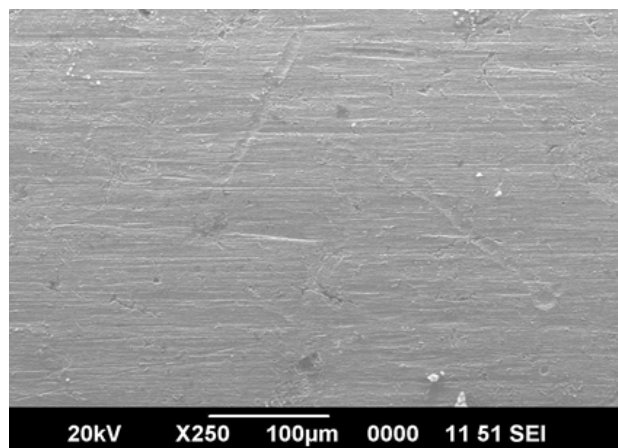


Fig:17. SEM image of mild steel after immersion in 1M HCl with *A.calcarata* rhizome extract 300ppm

3.13 / Fourier transform infrared spectroscopic studies (FTIR)

FT IR analysis helps to identify the functional groups present in the extracts and the corrosion product and to confirm the inhibition taking place due to the interaction between the extract and metal.

Figure 18 shows spectrum of plant extract (red) and corrosion product (film formed on the surface of the mild steel) (black) in case of *A.calcarata* leaf extract and figure 19 shows spectrum of plant extract (black) and corrosion product (red) respectively. Corrosion product showed several peaks corresponding to plant extract indicating an adsorption of plant extract on mild steel. Shift in wave length of the corrosion product indicate interaction between mild steel and plant extract. Functional groups missing in the spectra of corrosion product indicate adsorption of the inhibitor might have occurred through these missing bonds.

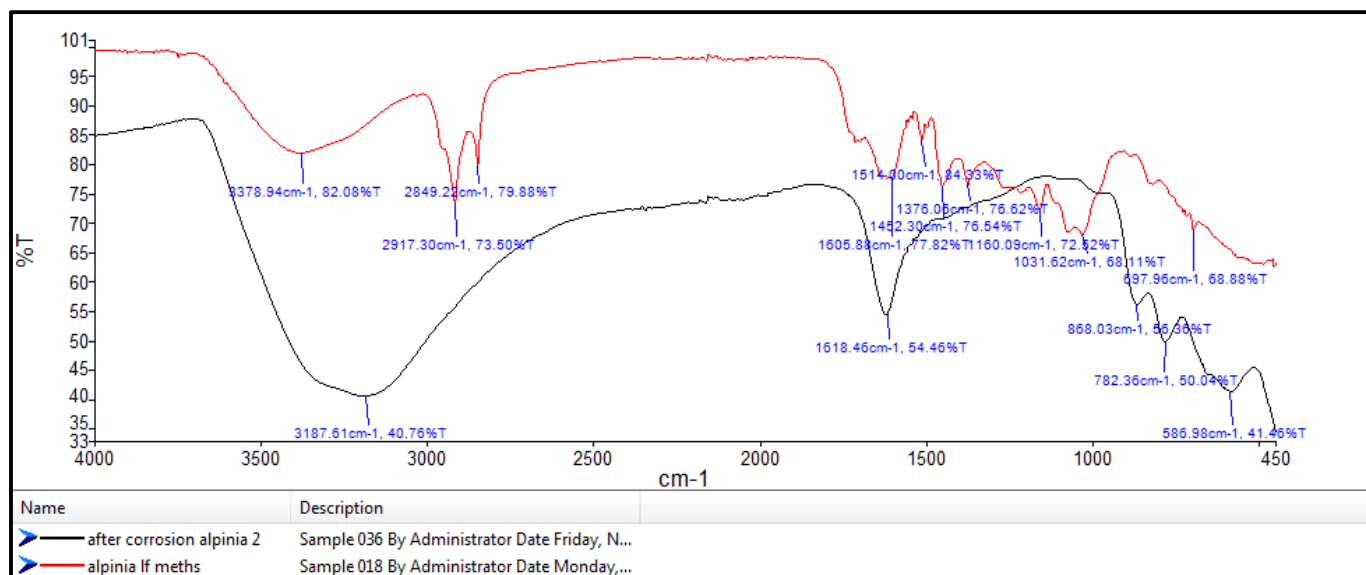


Fig :18. FT IR spectra of crude plant extract and corrosion product - *A.calcarata* leaf extract

3.14/ Antimicrobial activities

A.calcarata leaf and rhizome extract show considerably high antimicrobial activity against the organism tested. Zone of inhibition (ZI) (at 100µg/ml concentration) obtained against various tested organisms

are provided in table 13 and figures (20 -23) showing highest zone of inhibition against respective microbes are also provided. *A.calcarata* leaf methanolic extract show considerably good inhibition against *K. pneumoniae*, *S.mutans* and *C.albicans* repectively and leaf extracts are more efficient inhibitors than rhizome extracts.

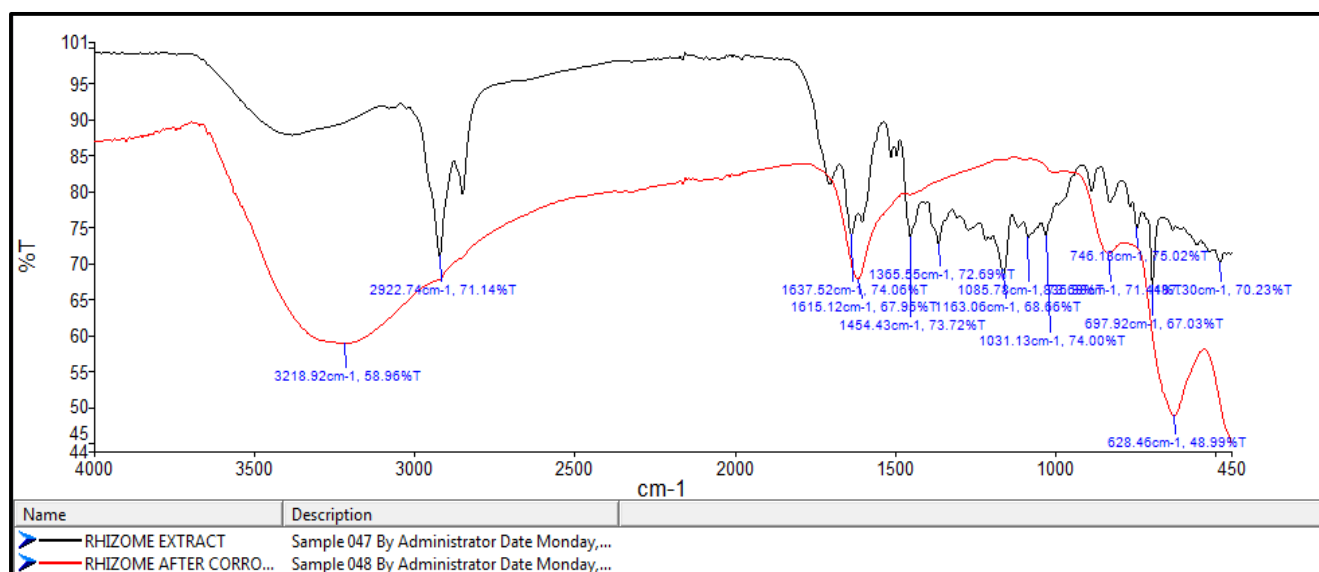


Fig :19. FT IR spectra of crude plant extract and corrosion product - *A.calcarata* rhizome extract

Table 13 . Antimicrobial activity of methanolic leaf and rhizome extracts of *A.calcarata*

Organism	Diameter of zone of inhibition (in mm)			
	<i>A.calcarata</i> leaf methanol extract		<i>A.calcarata</i> rhizome methanol extract	
	100 µg/ml	Control 20µg/ml	100 µg/ml	Control 20µg/ml
<i>Klebsiella pneumoniae</i>	38	37	16	37
<i>Pseudomonas aeruginosa</i>	27	40	20	40
<i>Streptococcus mutans</i>	36	40	17	40
<i>Staphylococcus aureus</i>	25	40	20	40
<i>Candida albicans</i>	37	39	15	39

3.15/ Molecular docking analysis

A. calcarata leaf and rhizome extracts showed good antimicrobial efficacy as revealed by in vitro studies. So in order to correlate *in vitro* and *in silico* results molecular docking studies were conducted. It effectively predicts the interaction between a ligand and a protein and thus is a crucial process in drug discovery. Different ligands are generally ranked as per their activity based on binding affinity values. The more negative the binding affinity greater the interaction between ligand and target protein. The results of docking analysis of selected phytochemicals from *A.calcarata* extracts with the target proteins are shown in table 14. The results are expressed as binding affinity values in Kcal/mol. From the results it can be concluded that the phytochemicals showed good interaction with the selected protein molecules. Highest binding interaction of penicillin binding protein 3 from *P. aeruginosa* was found with Benzene 1,3 dimethoxy -5-2 (phenyl ethenyl) - (E)- (from rhizome) with a binding affinity of -6.7 Kcal/mol. It was also observed that all the phytochemicals from rhizome selected for the present study interacted well with this protein. The glycerol dehydratase of *Klebsiella pneumoniae* effectively docked with a low

binding affinity value of -5.9 Kcal/mol by Cinnamic acid 4 hydroxy 3 methoxy methyl ester present in the methanolic extract of leaves. Stigmasterol showed the best interaction with inorganic pyrophosphatase of *S.mutans* with a binding affinity of -9.5 Kcal/mol (rhizome and leaf). Stigmasterol also showed good interaction with penicillin binding protein 3 from *P. aeruginosa* (-6.6 Kcal/mol), penicillin binding protein 2a from methcillin resistant *S. aureus* (-7.5 Kcal/mol) and protein geranylgeranyl transferase from fungi *C. albicans* (-6.1 Kcal/mol).



Fig: 20 *A.calcarata* leaf - *K.pneumoniae*



Fig: 21 *A.calcarata* leaf - *C.albicans*



Fig: 22 *A.calcarata* rhizome - *P.aeruginosa*



Fig: 23 *A.calcarata* rhizome - *S.aureus*

Highest binding interaction with penicillin binding protein 2a from methcillin resistant *S. aureus* was shown by Calcaratarin C present in methanolic extract of rhizome and Stigmasterol leaf and rhizome (both -7.5 Kcal/mol). The protein geranylgeranyl transferase from fungi *C. albicans* was found effectively inhibited by methanolic leaf and rhizome extracts with binding affinity value of -6.1 Kcal/mol for stigmasterol . Details of phytochemicals from different plant extracts used for docking analysis and molecular docking results of different phytochemicals with target proteins are provided in [table 14](#). Optimised geometry of certain phytochemicals and 3D diagrams regarding protein ligand interaction has also been provided in [fig. 24 - 31](#).

Table 14. Molecular docking results of different phytochemicals of *A.calcarata* leaf and rhizome with target proteins

Sl.No	Name of compound	Source	Binding affinity in Kcal/mol				
			Target proteins				
			<i>P.aeruginosa</i>	<i>K.pneumoniae</i>	<i>S.aureus</i>	<i>S.mutans</i>	<i>C.albicans</i>
1	Stigmasterol	leaf, rhizome	- 6.6		- 7.5	- 9.5	- 6.1
2	Daucol	rhizome	- 5		- 5.4		
3	Ambrial	rhizome	- 4.4		- 5.4		
4	Calcaratarin C	rhizome	- 6.5		- 7.5		
5	Benzene 1,3 dimethoxy-5-2(phenyl ethenyl)-(E)-	rhizome	- 6.7		- 6.5		
6	Cinnamic acid 4 hydroxy 3 methoxy methyl ester	leaf		- 5.9		- 6.5	- 6
7	2 methoxy 4 vinyl phenol	leaf		- 4.7		- 5.8	- 5.8
8	4- (2,2,6 - Trimethylcyclohexa-1,3 dienyl) but- 3- en-2-one	leaf		- 5.3		- 6.3	- 5.8
9	4 piperidone 2,2,6,6 tetramethyl	leaf		- 4.8		- 6	- 5

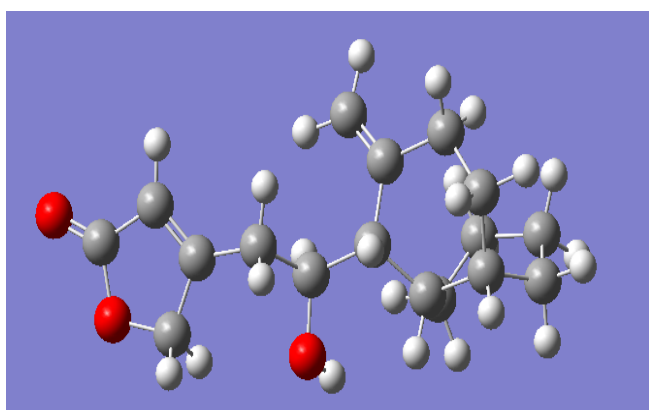


Fig. 24. Calcaratarin C

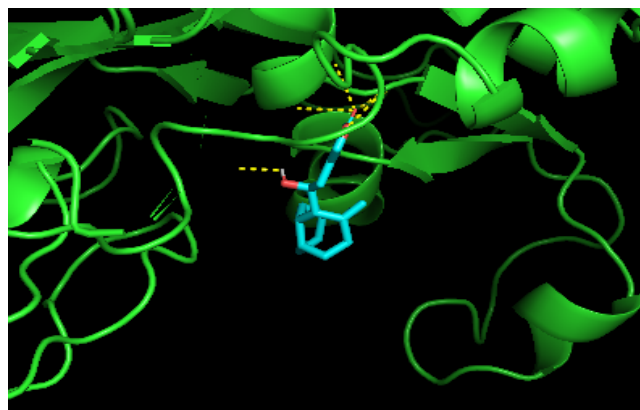


Fig.25. Interaction with protein from *S.aureus*

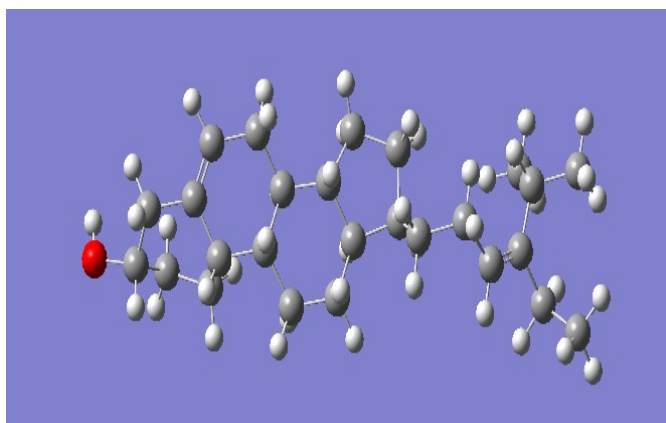


Fig.26. Stigmasterol

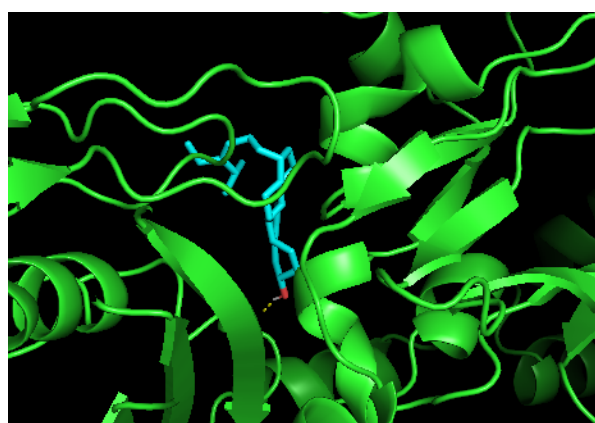


Fig. 27. Interaction with protein from *S.aureus*

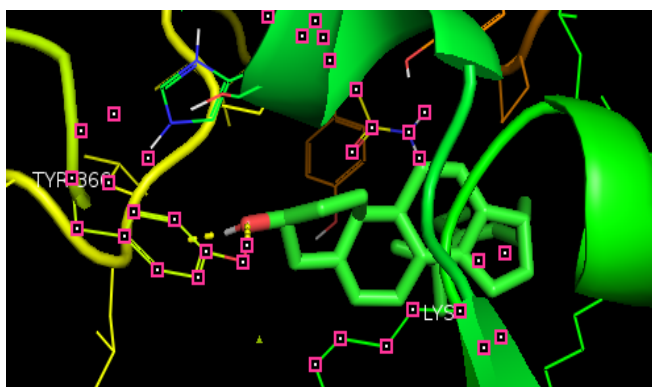


Fig. 28. Interaction with protein from *S.aureus*

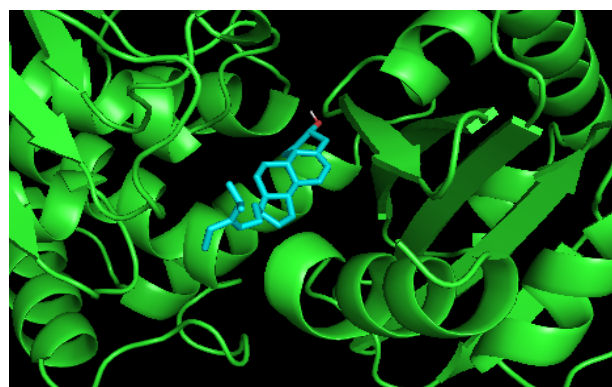


Fig.29. Interaction with protein from *S.mutans*

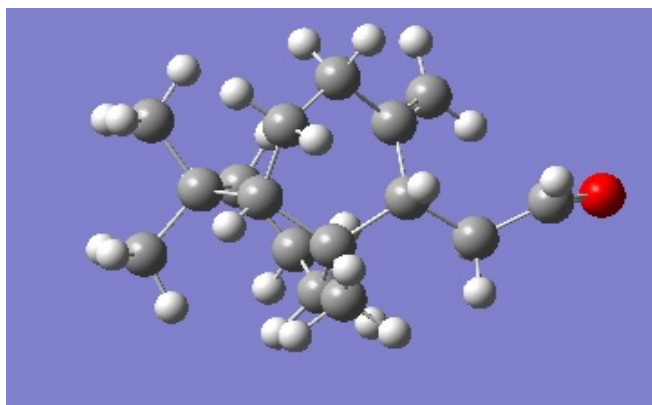


Fig. 30. Ambrial

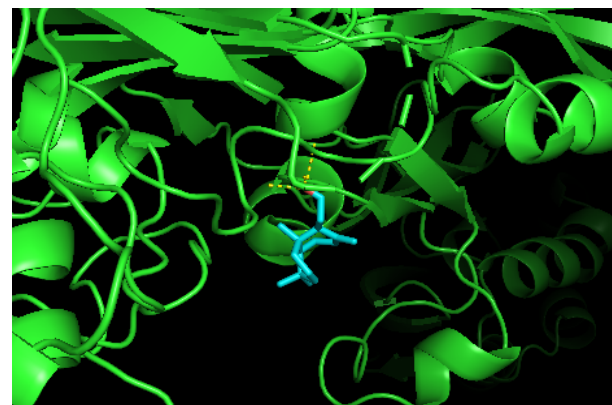


Fig. 31. Interaction with protein from *S.aureus*

Conclusion

The study revealed numerous phytoconstituents including some new compounds and total phenolics including flavonoids in the rhizome and leaf extracts of *A.calcarata*. Various antioxidant assays revealed significant antioxidant activity of the plant which has been supported by theoretical studies of some selected components of the plant. Experimental studies prove that *A.calcarata* rhizome and leaf extracts are very effective corrosion inhibitors of mild steel in 1 M HCl and both extracts are showing almost similar level of inhibition. FT-IR and SEM studies suggest the formation of protective barrier by extracts on mild steel surface. Adsorption of the extracts were further confirmed by experimental data fitting to Langmuir adsorption isotherm. DFT based quantum chemical computations of parameters associated with the electronic structures of some major selected components of plant extracts confirmed the inhibition potential of the plant extracts. Antimicrobial studies revealed considerably good inhibitory activity against the selected microbes. Molecular docking studies revealed that selected phytoconstituents exhibit good inhibitory interaction with the proteins of the microbes.

Acknowledgements - The first author is thankful to Kannur University for awarding a Junior Research Fellowship. The authors are grateful to the Principal and to the Head, Department of Chemistry, Sir Syed College, Taliparamba, Kannur for facilities.

References

1. P.S. Hema, Isolation and characterization of novel biologically active molecules. PhD thesis. Department of Chemistry, University of Kerala, (2009) 363 pp. <http://www.ir.niist.res.in>
2. Md. A. Rahman and Md.S. Islam, *Alpinia calcarata* Roscoe : A potential phytopharmacological source of natural medicine. *Pharmacogn. Rev.* 9(17) (2015) 55-62. <https://dx.doi.org/10.4103/0973-7847.156350>

3. L.S.R. Arambewela, L.D.A.M. Arawwawala, W.D. Ratnasooriya, Antinociceptive activities of aqueous and ethanolic extract of *Alpinia calcarata* rhizomes in rats. *J. Ethnopharmacol.* 95(2-3) (2004) 311-316.
4. K.R. Kirtikar & B.D. Basu, Indian Medicinal Plants, International Book Distributors, Dehradun, India. (1995) Vol 1. 371-372.
5. P.S. Varier, Indian Medicinal Plants - A compendium of 500 species. (1995) Vol. 1, p. 106
6. T.P. Prabhu, E. Selvakumari, V.S. Maheswaran, Pharmacognostical and preliminary phytochemical standardisation of rhizome *Alpinia calcarata* Rosc. *J. Pharmacog. Herb. Form.* 8: 2 (2012) 29 -34.
7. T.P. Prabhu, E. Selvakumari, V.S. Maheswaran, Suriyapadminimoka, S. Ragadeepthi, S.N. Alapatti, Phytochemical and antioxidant activity of ethanolic extract of *Alpinia calcarata* Rosc., *J. Pharm. Res* 1(3) (2012) 22 - 23.
8. R. Ramya, M. Kalaiselvi, R. Narmadha, D. Gomathi, V. Bhuvaneshwari, R. Amsaveni, K. Devaki, Secondary metabolite credentials and *in vitro* free radical scavenging activity of *Alpinia calcarata*. *J. Acute Med.* 5 (2015) 33 -3 <http://dx.doi.org/10.1016/j.jacme.2015.02.005>
9. L.Y. Kong, M. J. Qin, M. Niwa, Diterpenoids from the rhizomes of *Alpinia calcarata*, *J. Nat. Prod.*, 63 (2000) 939 - 942.
10. L.Y., Kong, Qin, M. J., M. Niwa, New cytotoxic bis-labdanic diterpenoids from *Alpinia calcarata*. *Planta Med.*, 68 (2002) 813 -817.
11. W-J. Zhang, J-G. Luo and L-Y. Kong, The Genus *Alpinia*: A Review of Its Phytochemistry and Pharmacology, *World J. Tradit. Chin. Med.* 2(1) (2016) 26-41, <http://dx.doi.org/0.15806/j.issn.2311-8571.2015.0026>
12. P. S. Hema, & M. S. Nair, Flavonoids and other constituents from the rhizomes of *Alpinia calcarata*. *Biochem. Syst. Ecol.* 37 (2009) 52 -54.
13. C.G. Sudha, M. George, K.B. Rameshkumar, G.M. Nair, Improved clonal propagation of *Alpinia calcarata* Rosc., a commercially important medicinal plant and evaluation of chemical fidelity through comparison of volatile compounds. *Am. J. Plant Sci.* 3 (2012) 930 -940.
14. P. Tripathi, & S.N. Swain, *In vitro* antioxidant and free radical scavenging activity of *Alpinia calcarata* in Andaman islands, *Plant Archives* 16 (2) (2016) 685 -694.
15. R. Perveen, H Ali, T Yeasmin, Antimicrobial and insecticidal activities of *Alpinia calcarata* rhizome. *Int. J. Pharma Sci. Res.* 1 (5) (2016) 48 -50.
16. J.P. Robinson, V Balakrishnan, J.S. Raj., S. J. Britto, Antimicrobial activity of *Alpinia calcarata* Rosc., and characterization of new α and β unsaturated carbonyl compounds. *Adv. Biol. Res.* 3 (5-6) (2009) 185 -187.
17. D. Bhunia, A.K. Mondal, Antibacterial activity of *Alpinia* L. (Zingiberaceae) from Santal and Lodha tribal areas of Paschim Medinipur district in Eastern India. *Adv. Bio Res.* 3 (2012) 54-63
18. J. George, Analysis of phytochemical constituents and antimicrobial activities of *Alpinia calcarata* against clinical pathogens. *Int. J. Pharma Sci. Res.* 5 (9) (2014) 555-560.
19. A. Hagerman, I. Muller, H. Makkar, Quantification of tannins in tree foliage. A laboratory manual. Vienna: FAO/IAEA, (2000) 4-7.
20. J. Zhishen, T. Mengcheng, W. Jianming. The determination of flavonoid contents in mulberry and their scavenging effects on superoxide radicals. *Food Chem.* 64 (1999) 555-559.
21. A. Braca, N.D. Tommasi, L.D. Bari, C. Pizza, M. Poloti, I. Morelli. Antioxidant principles from *Bauhinia tetrapotensis*. *J. Nat. Prod.* 64 (2001) 892 - 895.
22. M. Oyaizu, Studies on products of browning reactions: Antioxidative activities of products of browning reaction prepared from glucosamine. *Jpn. J. Nutr.* 44 (1986) 307 -315.

23. P. Prieto, M. Pineda, M. Anguilar, Spectrophotometric quantitation of antioxidant capacity through the formation of a phosphomolybdenum complex: Specific application to the determination of Vitamin E., *Anal Biochem.* 269 (1999) 337 - 341.
24. National committee for clinical laboratory standards. Performance standards for antimicrobial disk susceptibility tests - Fifth edition (1993): Approved Standard M2 -A5.NCCLS , Villanova, PA.
25. M.J. Frisch, G.W. Trucks, H.B. Schlegel, G.E. Scuseria, M.A. Rob, J. Cheeseman,.....D.J. Fox (2016): Gaussian 09; Revision A.02, Gaussian, Inc., Wallingford CT.
26. J.S. Binkley, J.A. Pople, W.J. Hehre, Self- consistent molecular orbital methods.21.Small split - valence basis sets for first row elements. *J. Am. Chem. Soc.*, 102 (1980) 939 -947.
<http://dx.doi.org/10.1021/ja00523a008>
27. J.E. Bartmess, Thermodynamics of the electron and proton. *J. Phys. Chem.* 98(25) (1994) 6420 - 6424
28. Q.V. Vo, P.C. Nam, M.V. Bay, N.M. Thong, N.D. Cuong, A. Mechler, Density functional theory study of the role of benzylic hydrogen atoms in the antioxidant properties of lignans. *Sci. Rep.* 8 (2018) 12361.1-10. <http://dx.doi.org/10.1038/s41598-018-30860-5>
29. A.M. Pisochi, A. Pop, C. Cimpeanu,G. Predoi, Antioxidant capacity determination in plants and plant - derived products: A review. *Oxid. Med. Cell. Longevity.* 3 (2016) 1-36.
30. A. El Bribri, M. Tabyaoui, B. Tabyaoui, H. El Attari, F. Bentiss, The use of *Euphorbia falcata* extract as ecofriendly corrosion inhibitor of carbon steel in hydrochloric acid solution. *Mater. Chem. Phys.* 141(1) (2013) 240 -247. <http://doi.org/10.1016/j.matchemphys.2013.05.006>
31. X. Li, S. Deng, H. Fu, Triazolyl blue tetrazolium bromide as a novel corrosion inhibitor for steel in HCl and H₂SO₄ solutions, *Corros. Sci.* 53 (2011) 302-309.
<https://doi.org/10.1016/j.corsci.2010.09.036>
32. G. Gece, Drugs: a review of promising novel corrosion inhibitors. *Corros. Sci.* 53 (2010) 3873 - 3893. <https://doi.org/10.1016/j.corsci.2011.08.006>
33. P.R. Ammal, R.P. Anupama, A. Joseph, Comparative studies on the electrochemical and physicochemical behaviour of three different benzimidazole motifs as corrosion inhibitor for mild steel in hydrochloric acid. *Egypt. J. Petrol.* 27 (2018) 1067 -1076.
<https://doi.org/10.1016/j.ejpe.2018.03.006>
34. G. Karthik & M. Sundaravadivelu, Studies on the inhibition of mild steel corrosion in hydrochloric acid solution by atenolol drug. *Egypt. J. Petrol.* 25 (2016) 183 -191.
<https://dx.doi.org/10.1016/e.ejpe.2015.04.003>
35. R. Mohan, K. Ramya, K.K. Anupama, A. Joseph, Density functional treatment and electroanalytical measurements of liquid phase interaction of 2-ethylbenzimidazole (EBI) and ethyl(2- ethylbenzimidazolyl) acetate (EEBA) on mild steel in hydrochloric acid. *J. Mol. Liq.* 220 (2016) 707 - 717. <https://doi.org/10.1016/j.molliq.2016.04.113>
36. K. Ramya & A.Joseph, Synergistic effects and hydrogen bonded interaction of alkyl benzimidazoles and thiourea pair on mildsteel in hydrochloric acid . *J. Taiwan Inst. Chem. Eng.* 52 (2015) 127 - 139. <http://dx.doi.org/10.1016/j.jtice.2015.01.027>
37. I. Lukowits, E. Kalman, F. Zucchi, Corrosion inhibitors - correlation between electronic structure and efficiency. *Corrosion* 57 (1) (2001) 3-8. <https://doi.org/10.5006/1.3290328>

(2021) ; <http://www.jmaterenvirosci.com>